Two-dimensional simulations of strongly radiating plasmas with the RALEF-2D code

M. M. Basko

Institute for Theoretical and Experimental Physics, Moscow

Moscow, November 30, 2009

Equations of hydrodynamics

One fluid, one temperature, two spatial dimensions (either x,y, or r,z):

$$\frac{\partial \rho}{\partial t} + \nabla \cdot \left(\rho \vec{u} \right) = 0,$$

$$\frac{\partial \left(\rho \vec{u} \right)}{\partial t} + \nabla \cdot \left(\rho \vec{u} \otimes \vec{u} \right) + \nabla p = 0,$$

$$\frac{\partial \left(\rho E \right)}{\partial t} + \nabla \cdot \left[\left(\rho E + p \right) \vec{u} \right] = \nabla \cdot \left(\kappa \nabla T \right) + Q_r + Q_{dep},$$

$$E = e + \frac{u^2}{2}, \quad e = e(\rho, T)$$

$\nabla \cdot \left(\kappa \nabla T \right)$ – energy deposition by thermal conduction (local), Q_r – energy deposition by radiation (non-local), Q_{dep} – eventual external heat sources.

Radiation transport

Transfer equation for radiation intensity I in the quasi-static approximation:

$$\cancel{\frac{1}{c}\frac{\partial I}{\partial t}} + \vec{\Omega}\cdot\nabla I = k_\nu\left(B_\nu - I\right), \quad I = I\left(t, \vec{x}, \nu, \vec{\Omega}\right), \quad B_\nu = B_\nu\left(\nu, T\right)$$

Quasi-static approximation: radiation transports energy infinitely fast (compared to the fluid motion) $\Rightarrow$ the energy residing in radiation field at any given time is infinitely small !

Coupling with the fluid energy equation:

$$Q_r = -\nabla\cdot\left(\int d\nu \int \vec{\Omega}\, I\, d\vec{\Omega}\right) = \int_{4\pi} d\vec{\Omega} \int k_\nu \left(I - B_\nu\right) d\nu$$

Radiation transport adds 3 extra dimensions (two angles and the photon frequency) $\Rightarrow$ **the 2D hydrodynamics becomes a 5D radiation hydrodynamics !**

Radiation transport in the diffusion approximation

In many cases the term “radiation hydrodynamics” is applied to hydrodynamic equations augmented with the multi-frequency diffusion equation

$$\frac{1}{c}\frac{\partial \mathfrak{A}_\nu}{\partial t} + \nabla\cdot\left(\mathfrak{A}_\nu \frac{\vec{u}}{c}\right) + \frac{1}{3}\mathfrak{A}_\nu \nabla\cdot\left(\frac{\vec{u}}{c}\right) = \nabla\cdot\left(\frac{1}{3k_\nu}\nabla\mathfrak{A}_\nu\right) + k_\nu\left(\frac{B_\nu}{c} - \mathfrak{A}_\nu\right)$$

for the spectral radiation energy density $\mathfrak{A}_\nu$; the radiation diffusion equation is coupled to the fluid energy equation via the energy exchange term

$$Q_r = \int k_\nu \left(c\mathfrak{A}_\nu - B_\nu\right) d\nu \ .$$

In this treatment, information about the angular dependence of the radiation field is lost (e.g. the CHIC code, P.-H. Maire, J. Breil), and the 2D hydrodynamics becomes a 3D radiation hydrodynamics.

Whereas finite-difference treatment of the <u>multi-frequency diffusion</u> is similar to that of thermal conduction, solution of the transport equation requires a completely different numerical scheme.

Numerical scheme for hydrodynamics

To solve numerically the equations of hydrodynamics in two dimensions, we employ the CAVEAT-2D (LANL, 1990) hydrodynamics package. The CAVEAT numerical scheme has the following properties:

- it uses cell-centered principal variables on a multi-block structured quadrilateral mesh (either in the x-y or r-z geometry);
- is fully conservative and belongs to the class of second-order Godunov schemes;
- the mesh is adapted to the hydrodynamic flow by applying the ALE (arbitrary Lagrangian-Eulerian) technique;
- the numerical method is based on a fast non-iterative Riemann solver (J.K.Dukowicz, 1985), easily applied to arbitrary equation of state.

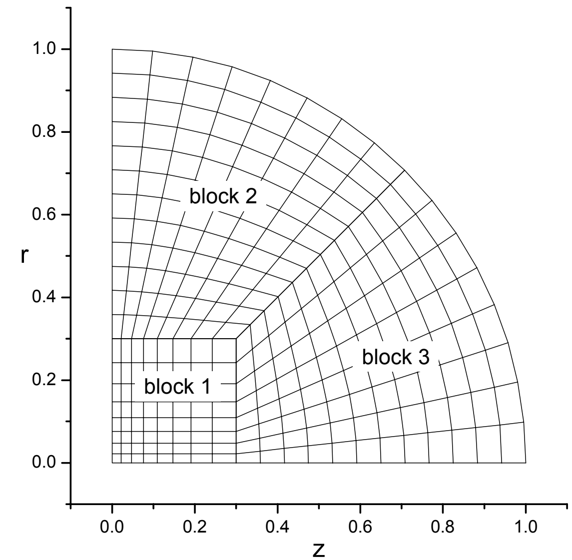

Numerical scheme for thermal conduction

The key ingredient to the RALEF-2D code is the **SSI (symmetric semi-implicit)** method of E.Livne & A.Glasner (1985), used to incorporate **thermal conduction** and **radiation transport** into the 2D Godunov method.

The numerical scheme for thermal conduction (M.Basko, J.Maruhn & A.Tauschwitz, J.Com.Phys., **228**, 2175, 2009) has the following features:

- it uses cell-centered temperatures from the FVD (finite volume discretization) hydrodynamics on distorted quadrilateral grids,
- is fully conservative (based on intercellular fluxes with an SSI energy correction for the next time step),
- (almost) unconditionally stable,
- space second-order accurate on all grids for smooth κ,
- symmetric on a local 9-point stencil,
- computationally efficient.

Numerical scheme for radiation transport

Our numerical scheme for radiation transport (not published yet) has the following basic properties:

- radiation coupling to the fluid is combined with thermal conduction within the unified **SSI approach**;
- the angular dependence is treated by applying the classical **S_n method** with n(n+2) fixed photon propagation directions over the 4π solid angle;
- the scheme is **non-conservative** in the sense that energy deposition by radiation Q_r is calculated not via elementary fluxes,
- the algorithm has the important property of correct transition to **the diffusion limit** when mesh cells become optically thick.

Presently, we do not see any practical alternative to the SSI method to cope with numerical instabilities in cases where radiation transport has a strong dynamic impact on hydrodynamics.

The method of short characteristics

For each angular direction $\vec{\Omega}_L$ and frequency ν, the radiation field I is found by solving the transfer equation

$$\vec{\Omega}_L \cdot \nabla I = k_\nu \left(B_\nu - I\right), \qquad I = I\left(t, \vec{x}, \nu, \vec{\Omega}_L\right),$$

with the **method of short characteristics** (A.Dedner, P.Vollmöller, JCP, **178**, 263, 2002). **Mesh nodes** are chosen as collocation points for the radiation intensity I.

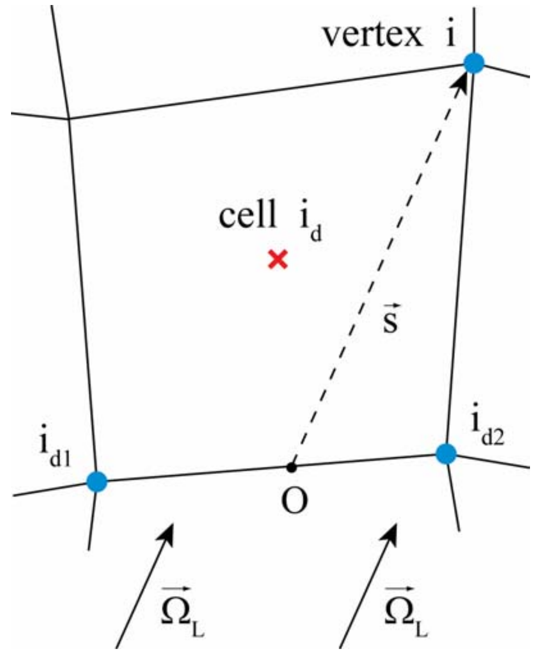

Advantages:

- even on strongly distorted meshes, it is guaranteed that light rays pass through each mesh cell;
- the algorithm is generally computationally more efficient than that of long characteristics.

Disadvantages:

- a significant amount of numerical diffusion in space.

Difference with R.Ramis: in the MULTI-2D code I is assigned to cell edges.

Only Cartesian geometry with straight characteristics has been treated so far.

Numerical diffusion: a searchlight beam in vacuum

The method of short characteristics produces a significant amount of numerical diffusion for light beams with sharp edges.

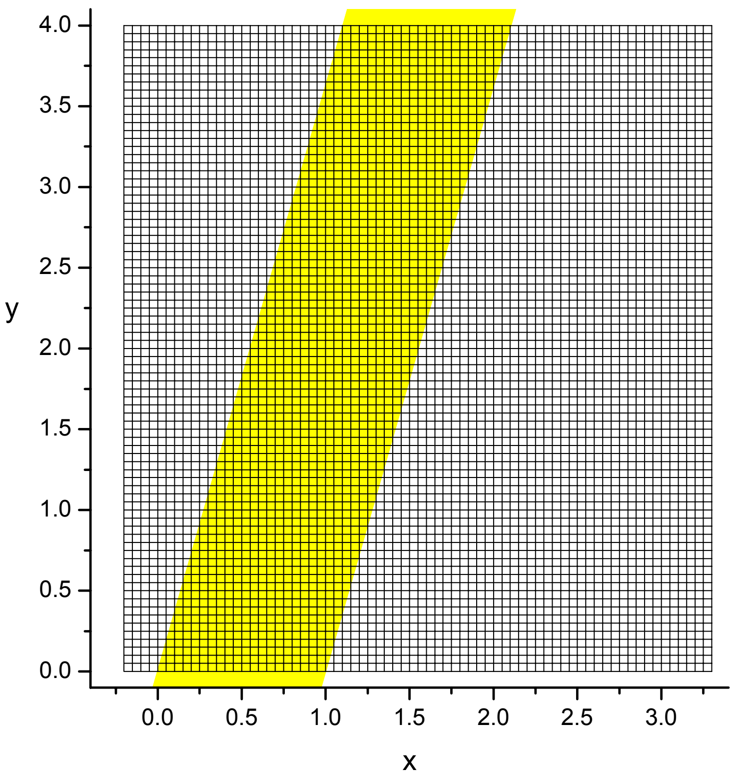

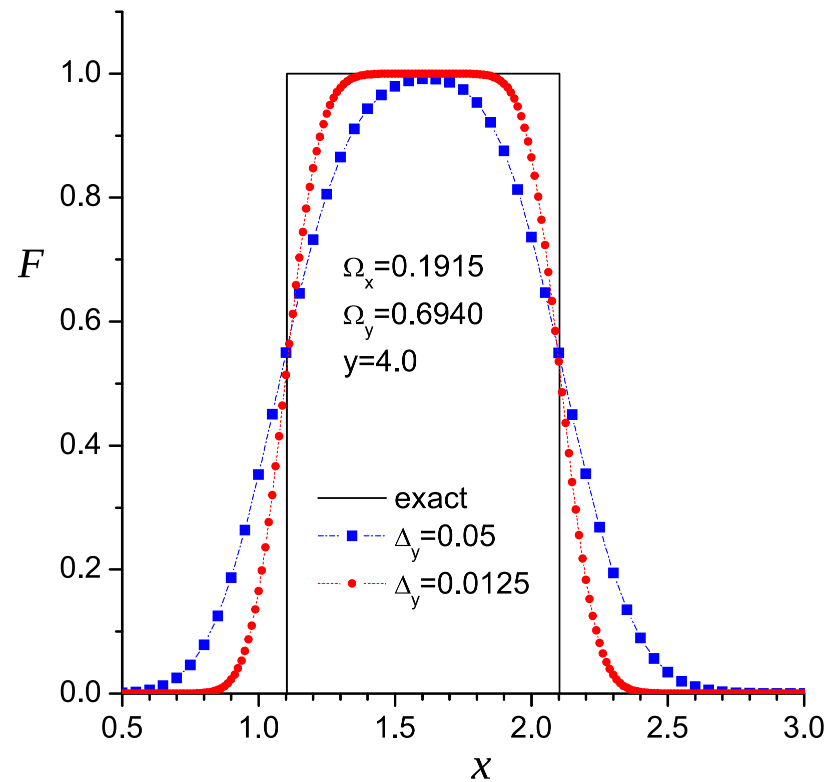

However, for thermal radiation a certain amount of numerical diffusion may be more an advantage than a shortcoming.

Vital importance of the ALE technique

The problem: a thin foil is irradiated by an intense laser beam.

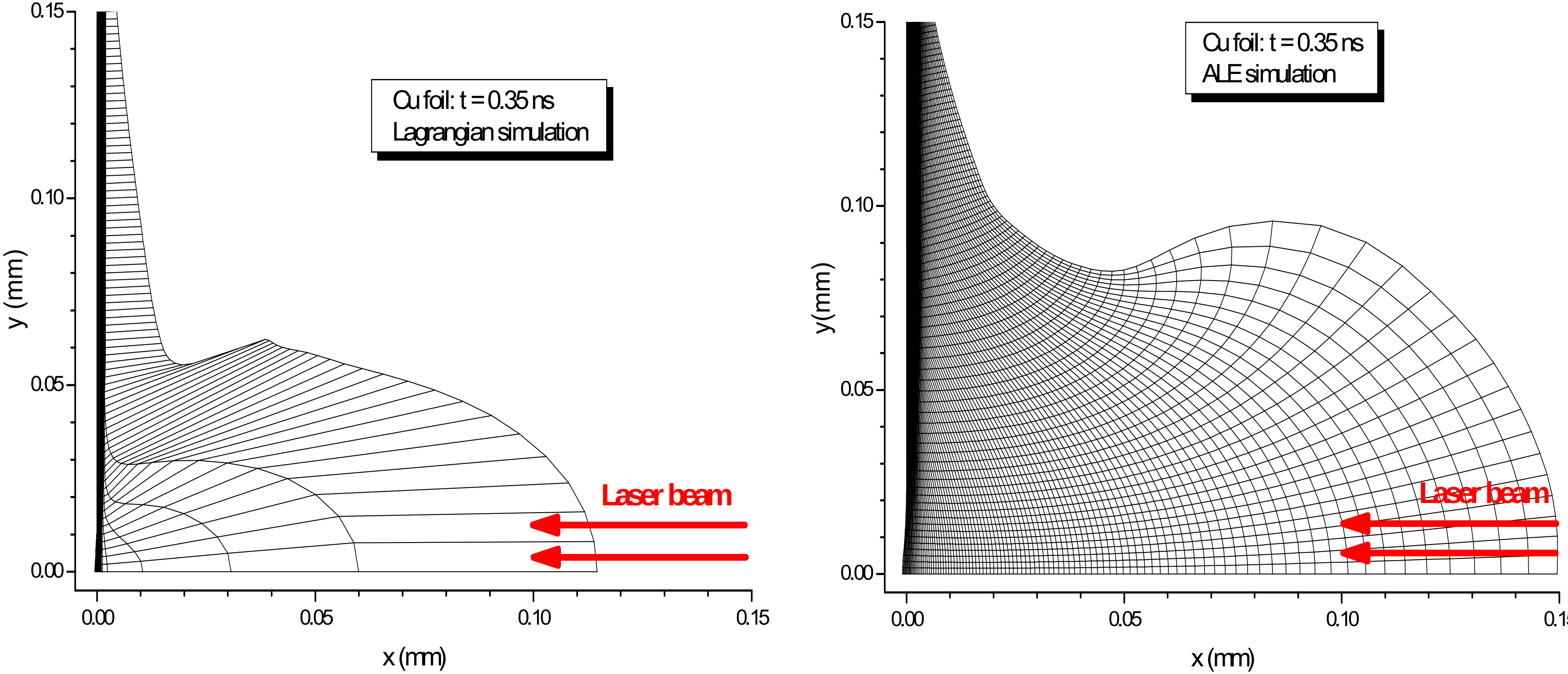

Problem 1: A strongly radiating central Z-pinch in tungsten multi-wire arrays

Multi-wire Z-pinches (Sandia, Angara-5)

40-mm diameter array of 240, 7.5-μm-diam. wires.

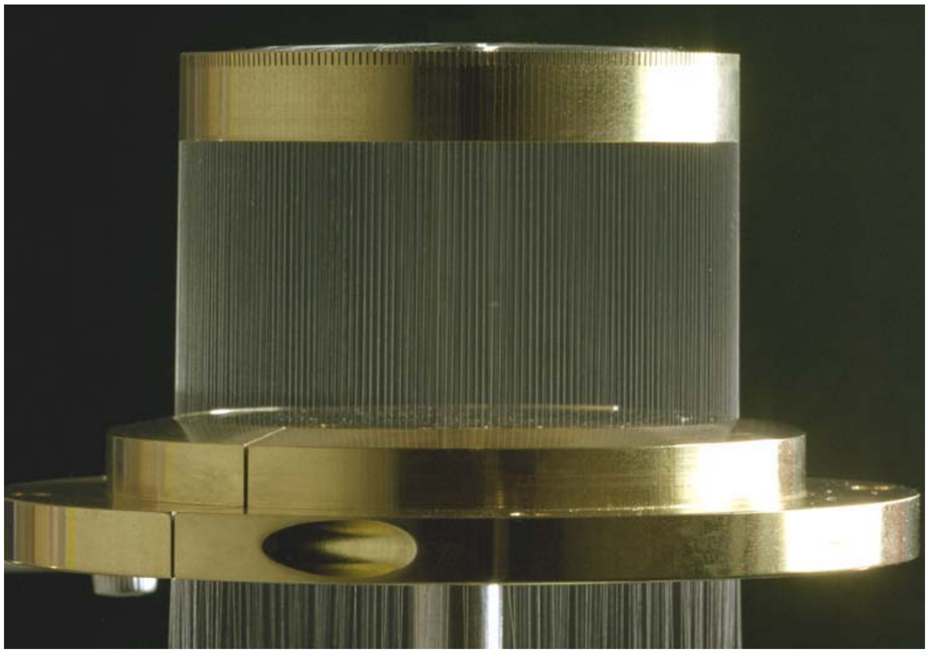

<u>Z-machine at Sandia (USA):</u>

- **11.5 MJ stored energy**
- **19 MA peak load current**
- **40 TW electrical power to load**
- **100-250 TW x-ray power**
- **1-1.8 MJ x-ray energy**

Problem statement for the Angara-5 parameters

Cylindrical implosion of an initially cold tungsten plasma cloud

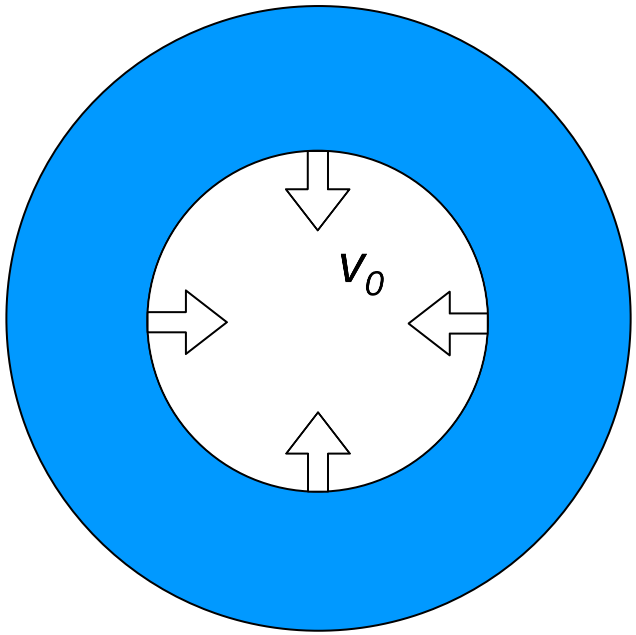

Initial shell parameters:

- radial thickness 2 mm;
- implosion velocity v_0 = 400 km/s;
- uniform temperature T_0 = 20 eV;
- mass per unit length 0.286 mg/cm;
- initial kinetic energy 23 kJ/cm;
- far from the axis, mass is uniformly distributed over the radius;
- possible influence of magnetic field is neglected.

In its present formulation, the problem is one-dimensional.

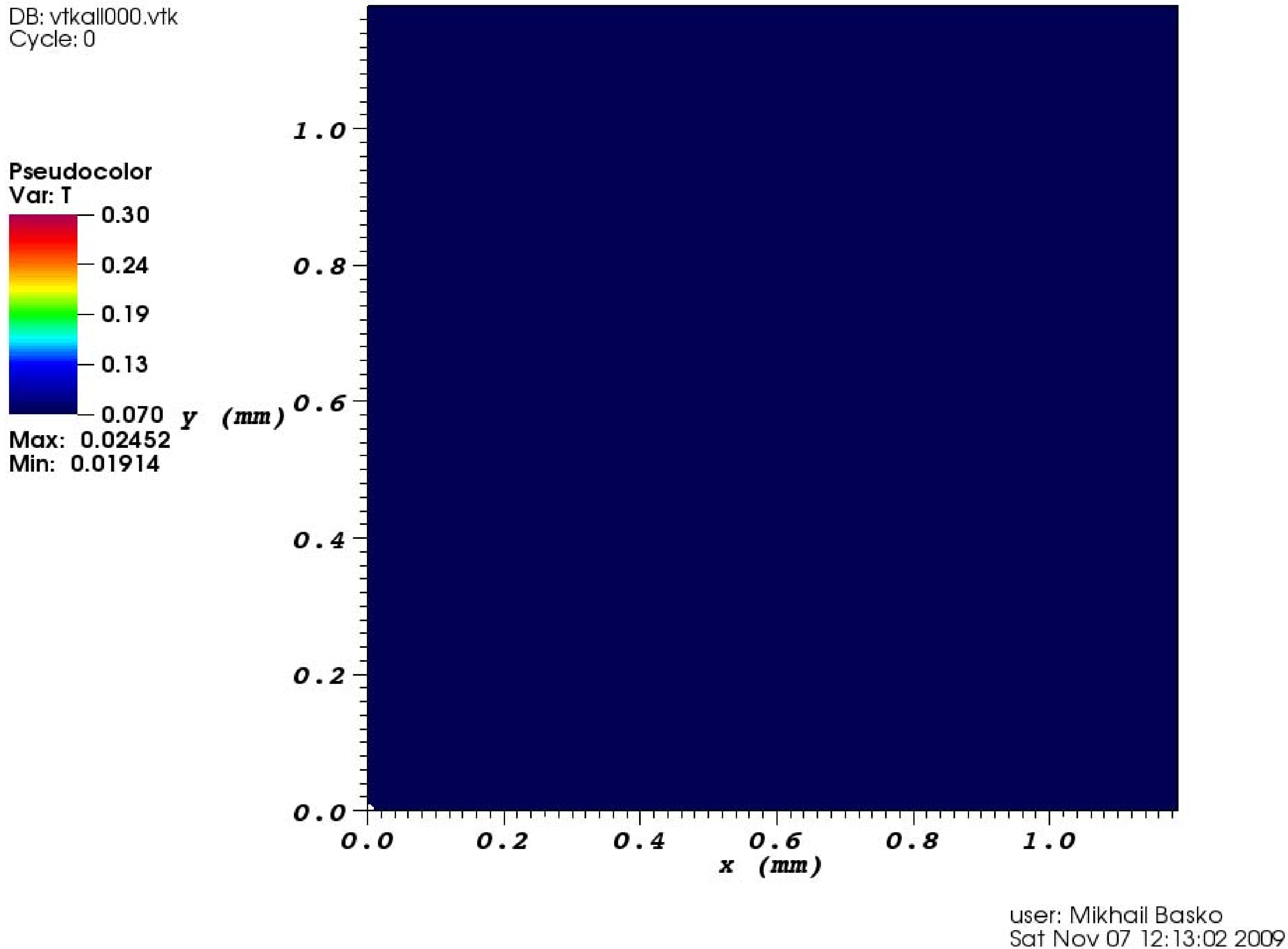
DB: vtkall000.vtk
Cycle: 0
Pseudocolor
Var: T
0.30
0.24
0.19
0.13
0.070
Max: 0.02452
Min: 0.01914
y (mm)
1.0
0.8
0.6
0.4
0.2
0.0
0.0
0.2
0.4
0.6
0.8
1.0
x (mm)
user: Mikhail Basko
Sat Nov 07 12:13:02 2009

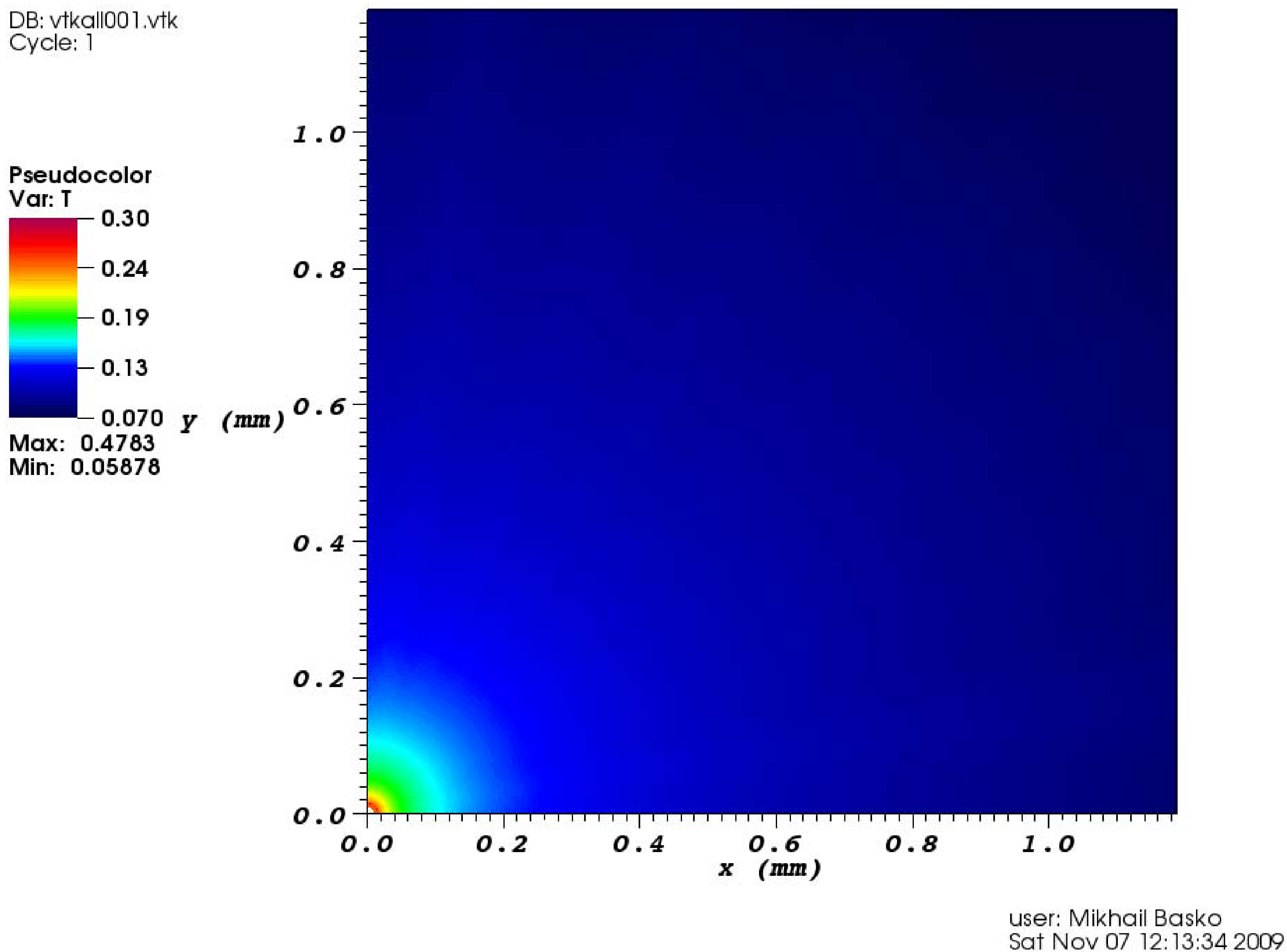
DB: vtkall001.vtk
Cycle: 1
Pseudocolor
Var: T
0.30
0.24
0.19
0.13
0.070
Max: 0.4783
Min: 0.05878
y (mm)
1.0
0.8
0.6
0.4
0.2
0.0
0.0
0.2
0.4
0.6
0.8
1.0
x (mm)
user: Mikhail Basko
Sat Nov 07 12:13:34 2009

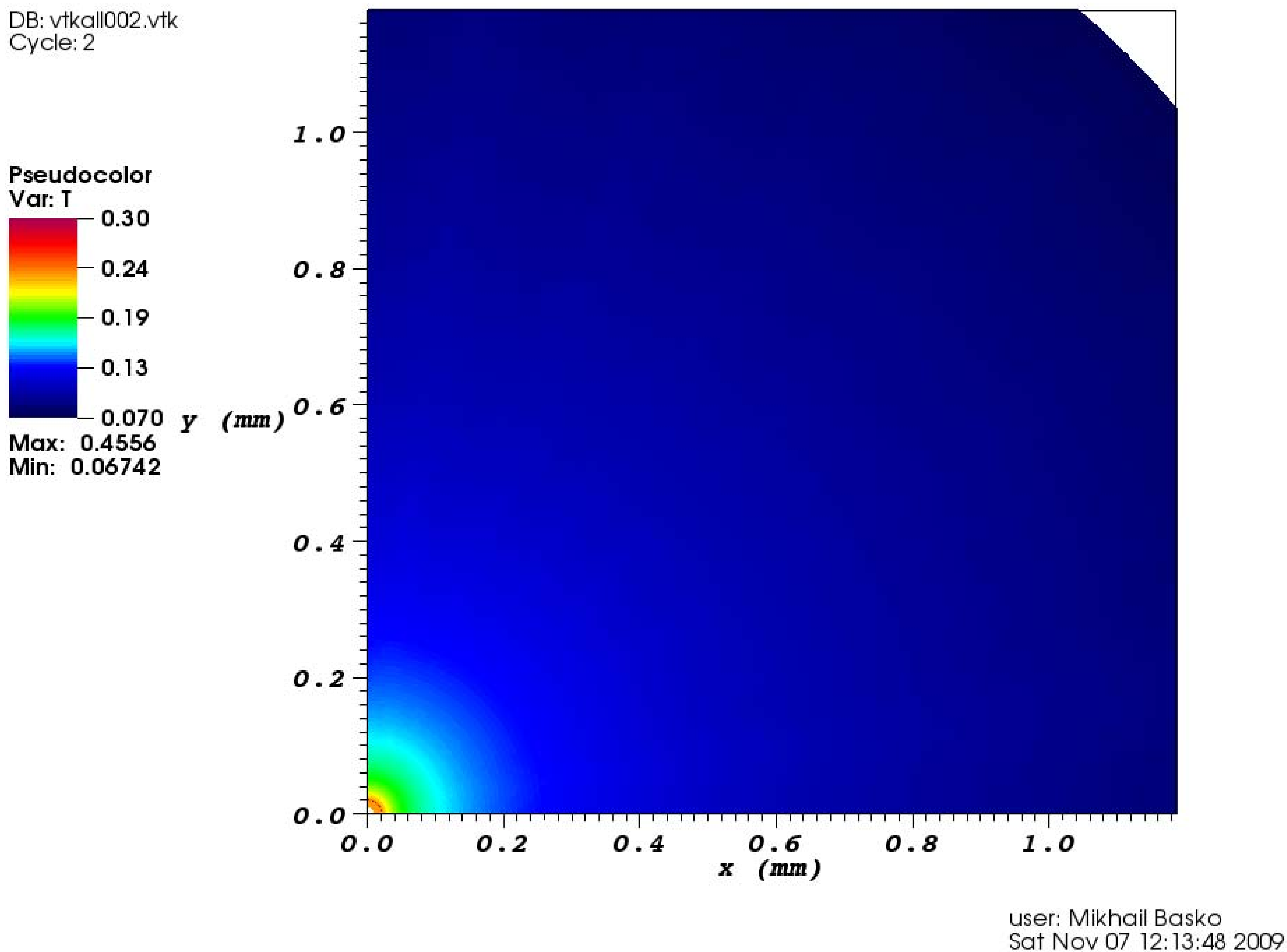

DB: vtkall002.vtk
Cycle: 2
Pseudocolor
Var: T
0.30
0.24
0.19
0.13
0.070
Max: 0.4556
Min: 0.06742
y (mm)
1.0
0.8
0.6
0.4
0.2
0.0
0.0
0.2
0.4
0.6
0.8
1.0
x (mm)
user: Mikhail Basko
Sat Nov 07 12:13:48 2009

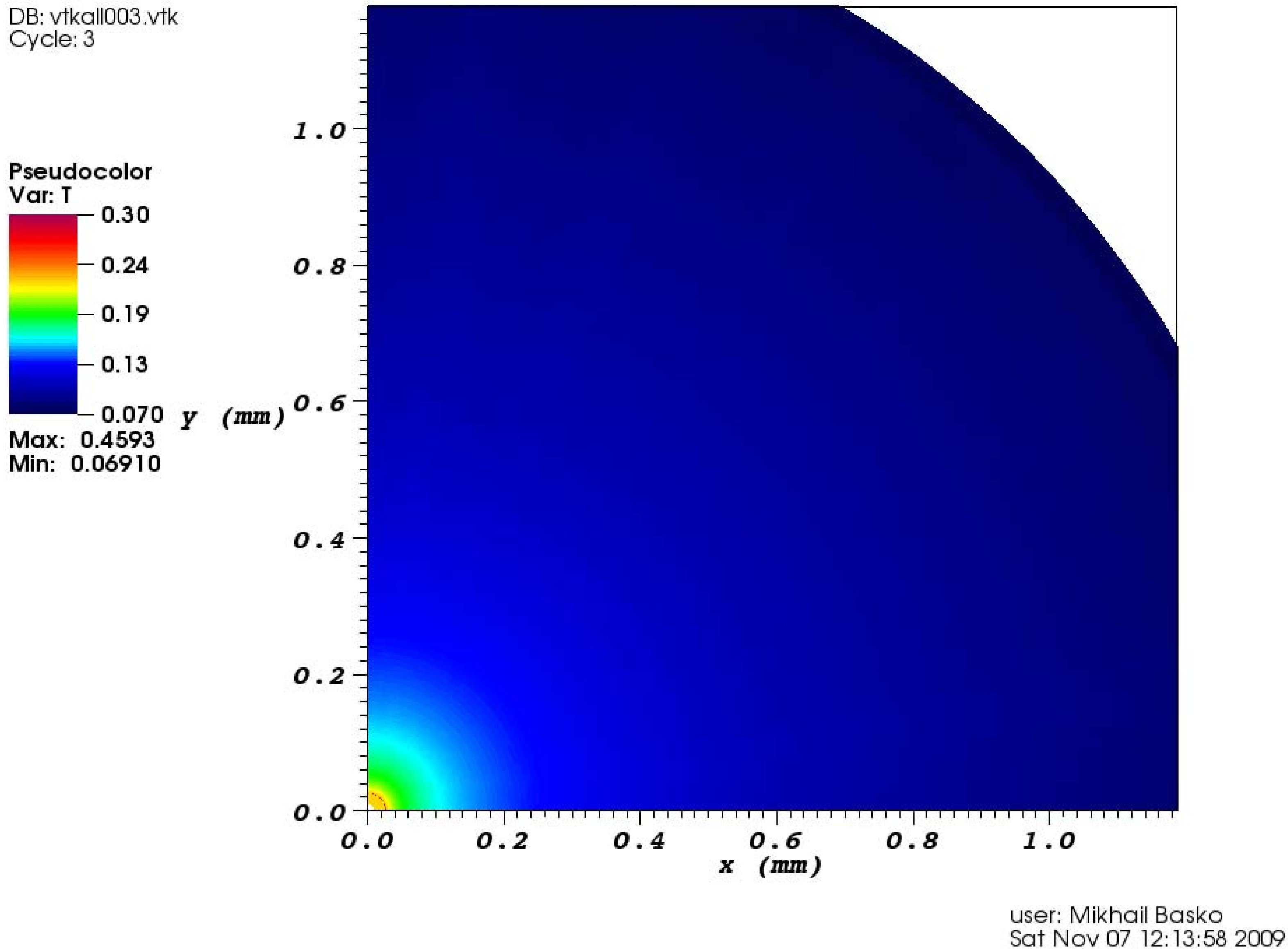
DB: vtkall003.vtk
Cycle: 3
Pseudocolor
Var: T
0.30
0.24
0.19
0.13
0.070
Max: 0.4593
Min: 0.06910
y (mm)
1.0
0.8
0.6
0.4
0.2
0.0
0.0
0.2
0.4
0.6
0.8
1.0
x (mm)
user: Mikhail Basko
Sat Nov 07 12:13:58 2009

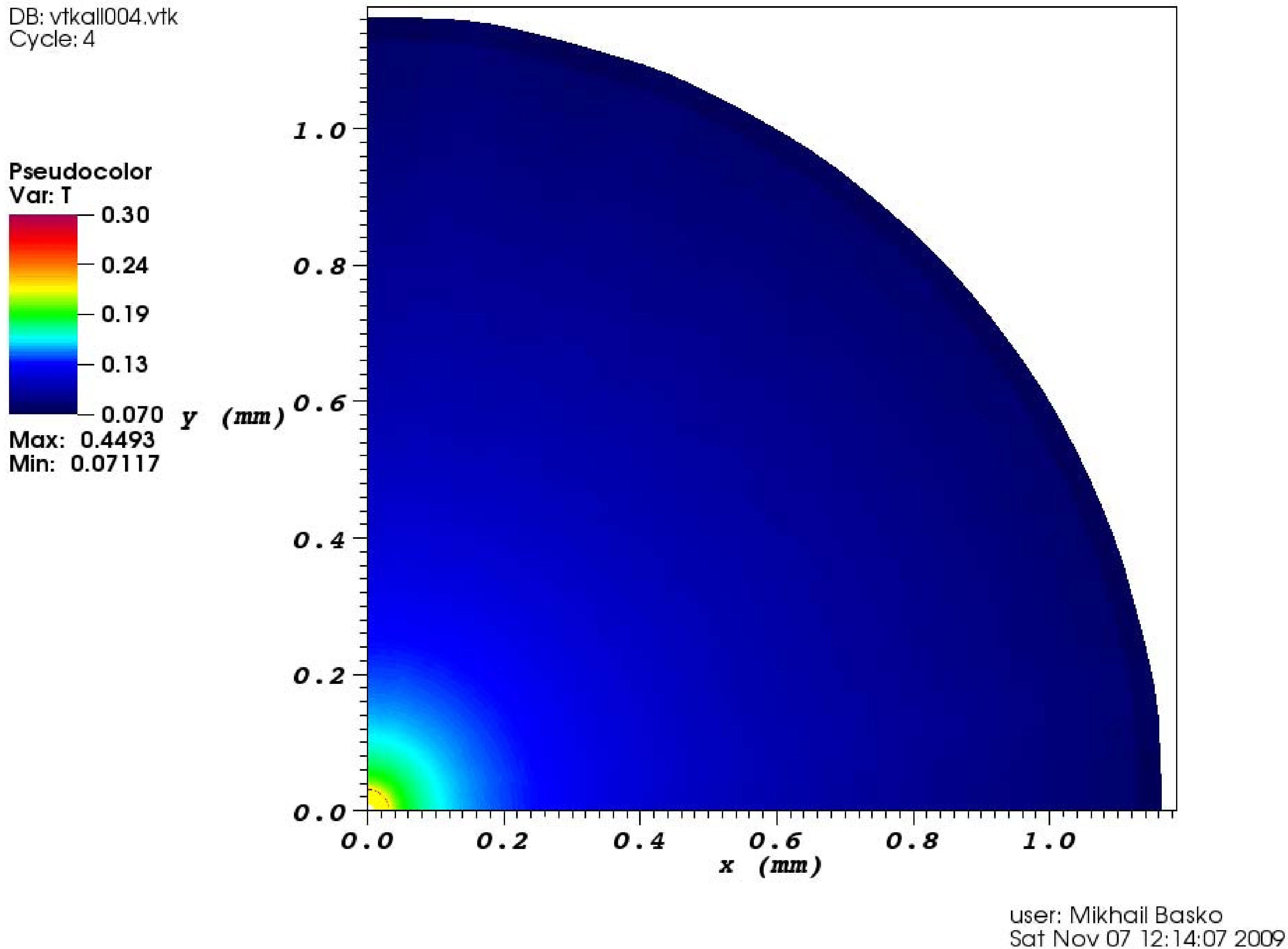
DB: vtkall004.vtk
Cycle: 4
Pseudocolor
Var: T
0.30
0.24
0.19
0.13
0.070
Max: 0.4493
Min: 0.07117
y (mm)
1.0
0.8
0.6
0.4
0.2
0.0
0.0
0.2
0.4
0.6
0.8
1.0
x (mm)
user: Mikhail Basko
Sat Nov 07 12:14:07 2009

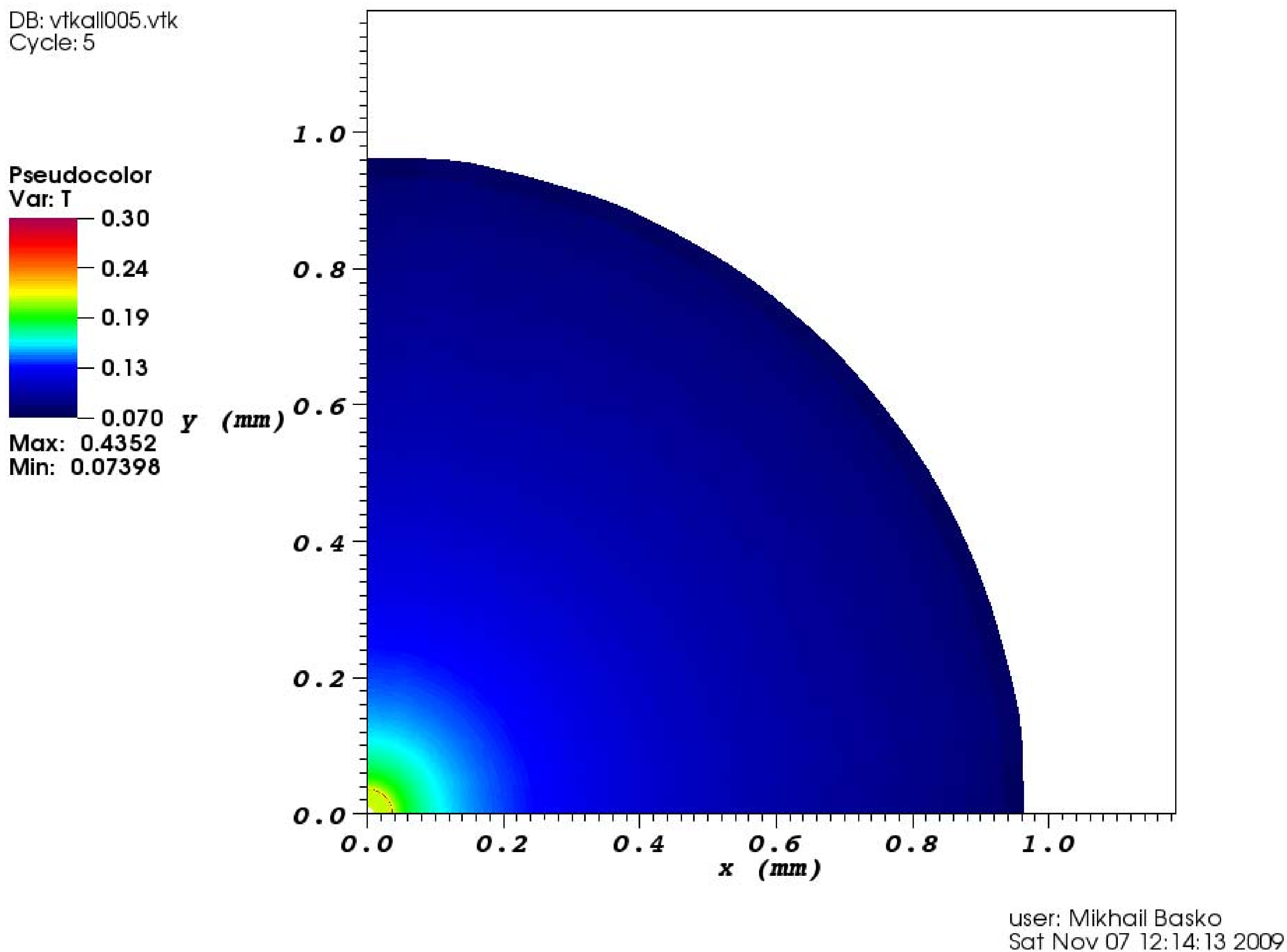
DB: vtkall005.vtk
Cycle: 5
Pseudocolor
Var: T
0.30
0.24
0.19
0.13
0.070
Max: 0.4352
Min: 0.07398
y (mm)
1.0
0.8
0.6
0.4
0.2
0.0
0.0
0.2
0.4
0.6
0.8
1.0
x (mm)
user: Mikhail Basko
Sat Nov 07 12:14:13 2009

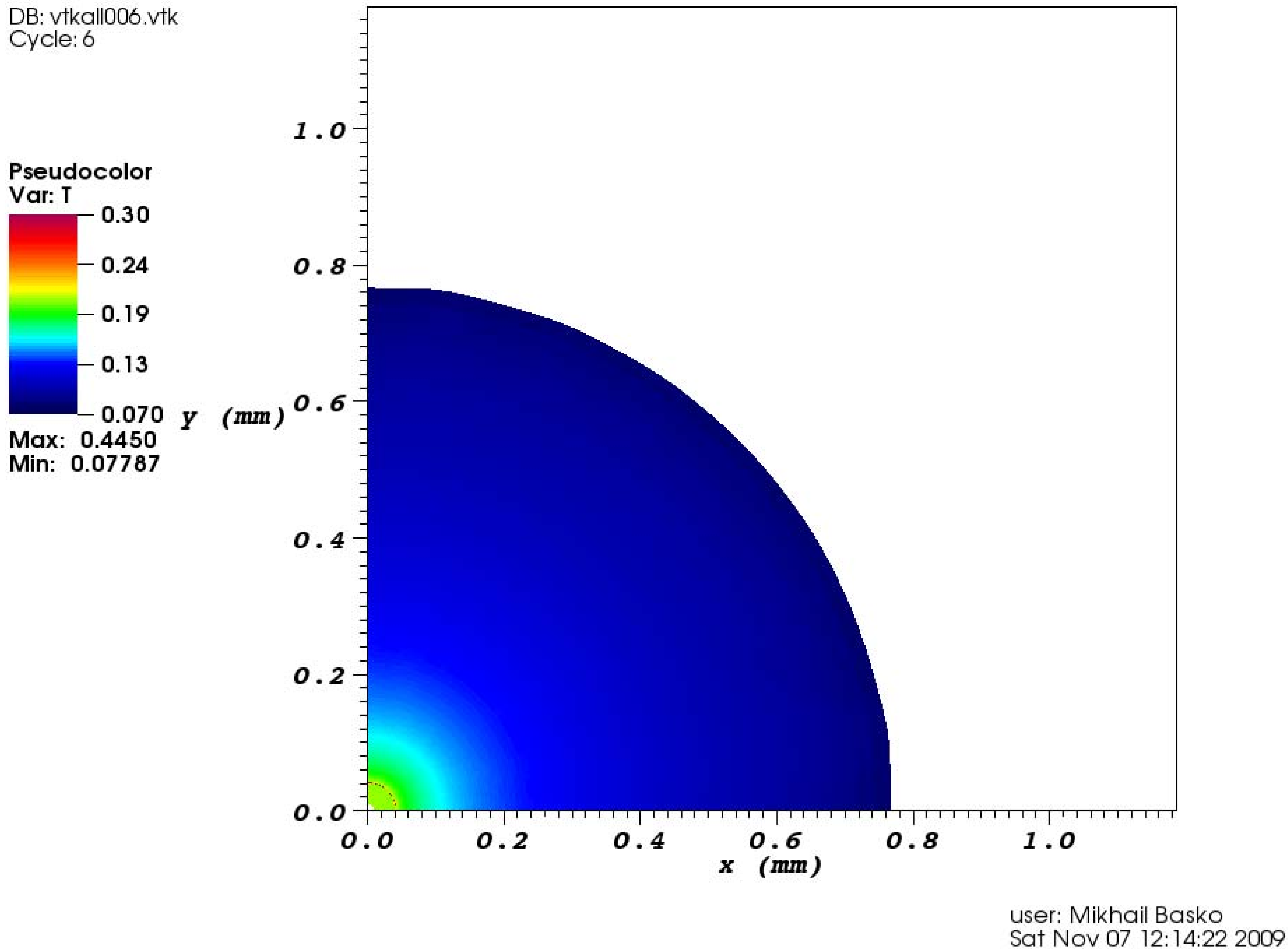
DB: vtkall006.vtk
Cycle: 6
Pseudocolor
Var: T
0.30
0.24
0.19
0.13
0.070
Max: 0.4450
Min: 0.07787
y (mm)
1.0
0.8
0.6
0.4
0.2
0.0
0.0
0.2
0.4
0.6
0.8
1.0
x (mm)
user: Mikhail Basko
Sat Nov 07 12:14:22 2009

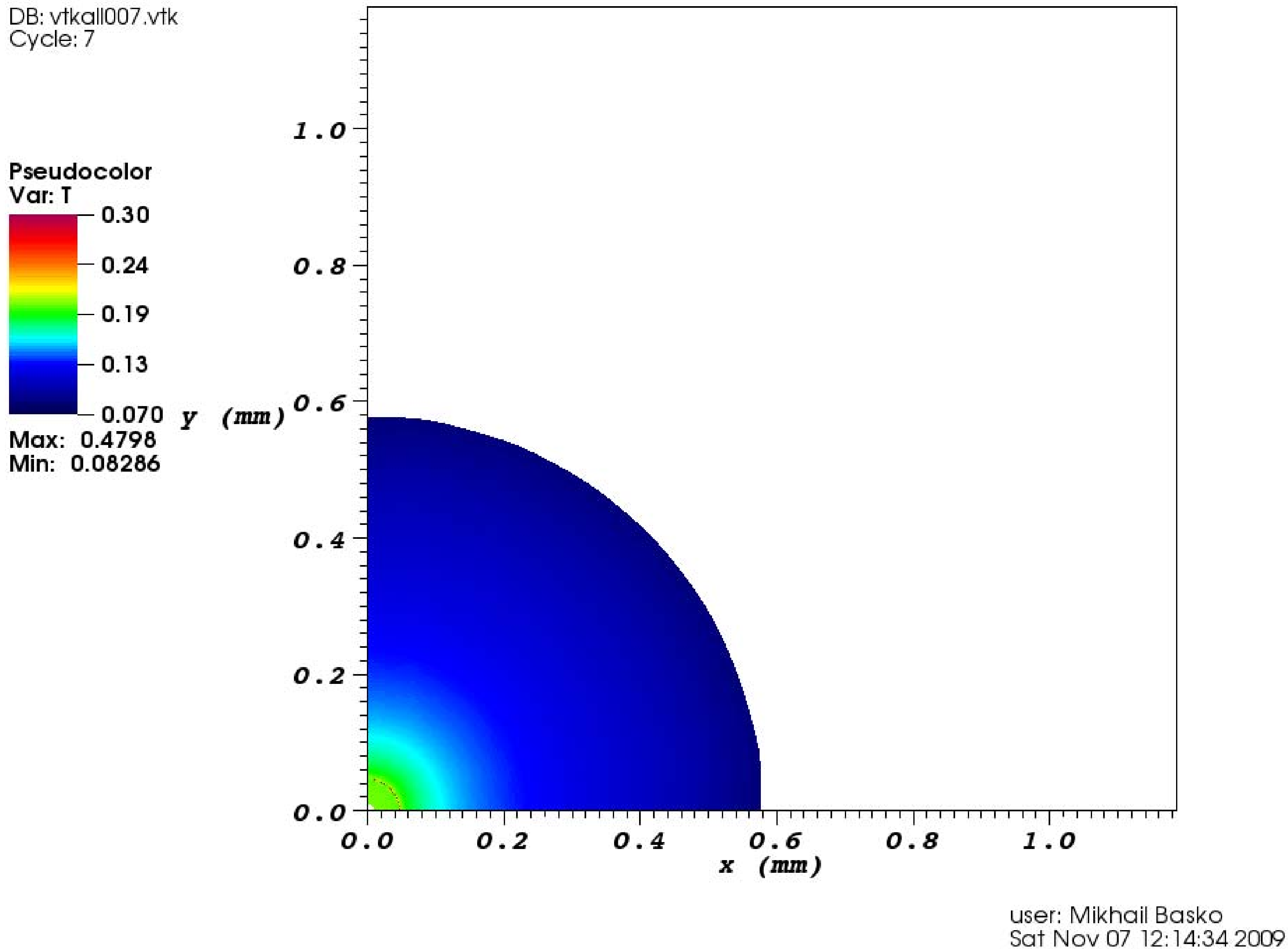
DB: vtkall007.vtk
Cycle: 7
Pseudocolor
Var: T
0.30
0.24
0.19
0.13
0.070
Max: 0.4798
Min: 0.08286
y (mm)
x (mm)
0.0
0.2
0.4
0.6
0.8
1.0
user: Mikhail Basko
Sat Nov 07 12:14:34 2009

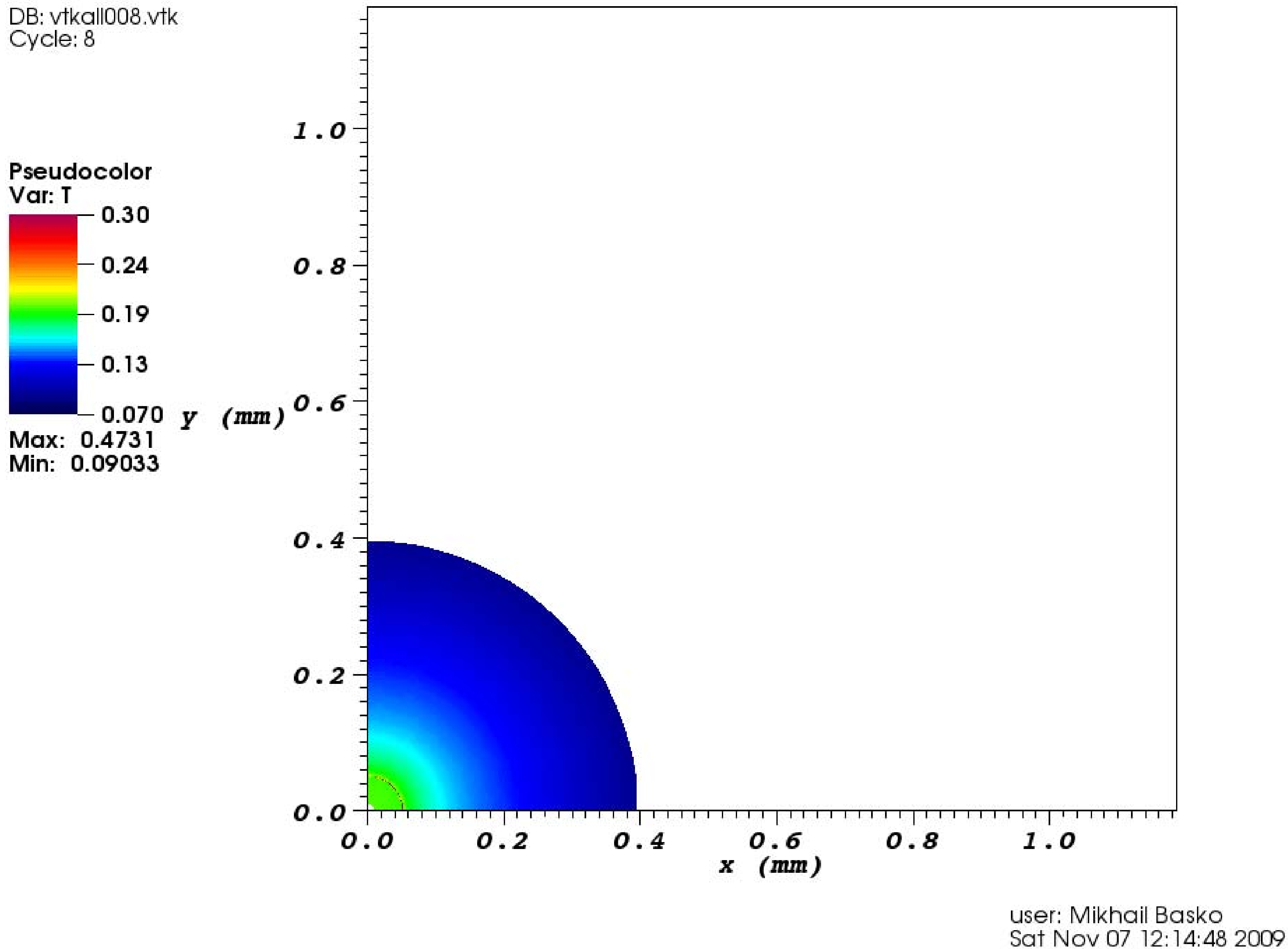
DB: vtkall008.vtk
Cycle: 8
Pseudocolor
Var: T
0.30
0.24
0.19
0.13
0.070
Max: 0.4731
Min: 0.09033
y (mm)
1.0
0.8
0.6
0.4
0.2
0.0
0.0
0.2
0.4
0.6
0.8
1.0
x (mm)
user: Mikhail Basko
Sat Nov 07 12:14:48 2009

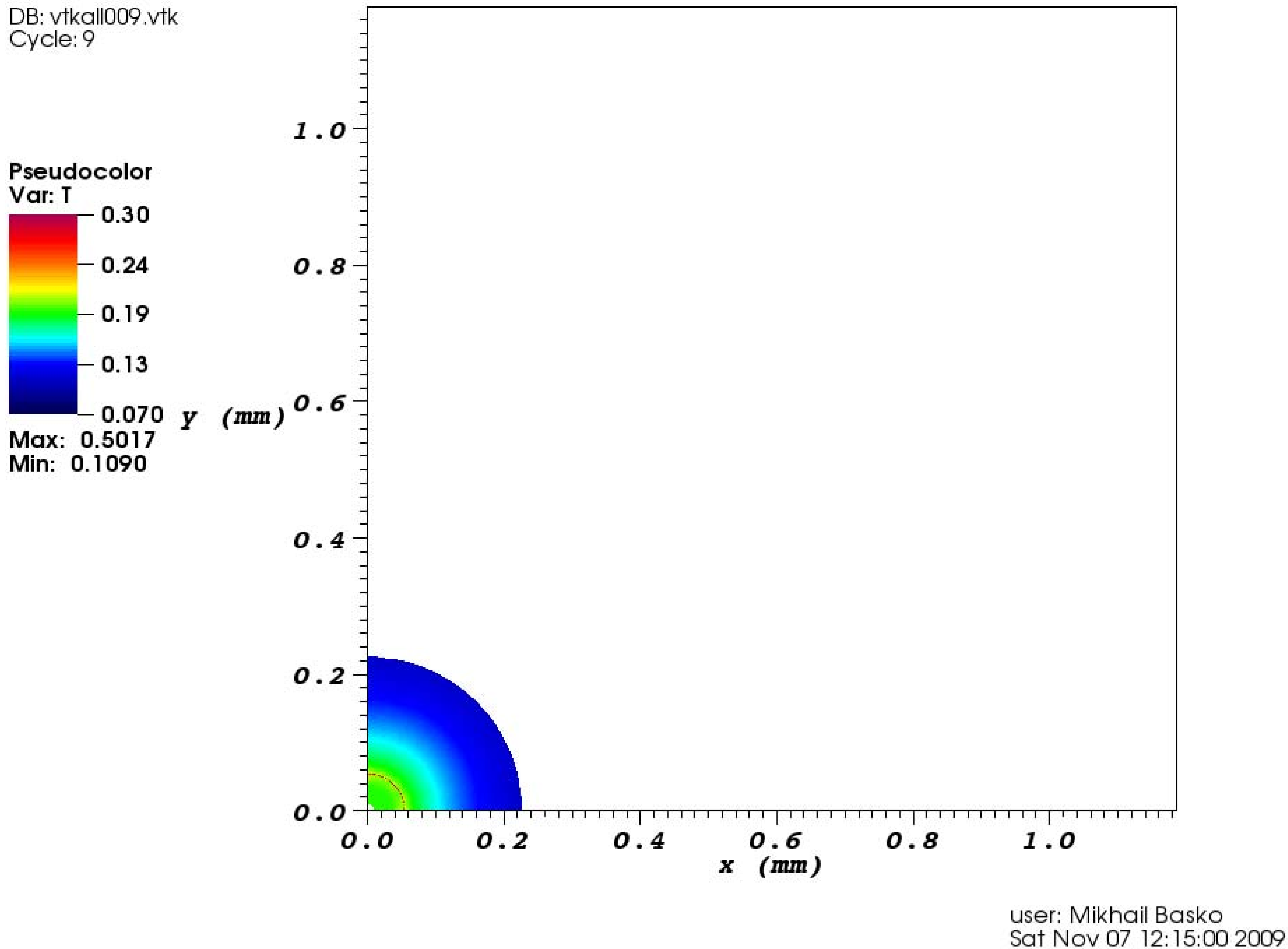
DB: vtkall009.vtk
Cycle: 9
Pseudocolor
Var: T
0.30
0.24
0.19
0.13
0.070
Max: 0.5017
Min: 0.1090
y (mm)
x (mm)
0.0
0.2
0.4
0.6
0.8
1.0
user: Mikhail Basko
Sat Nov 07 12:15:00 2009

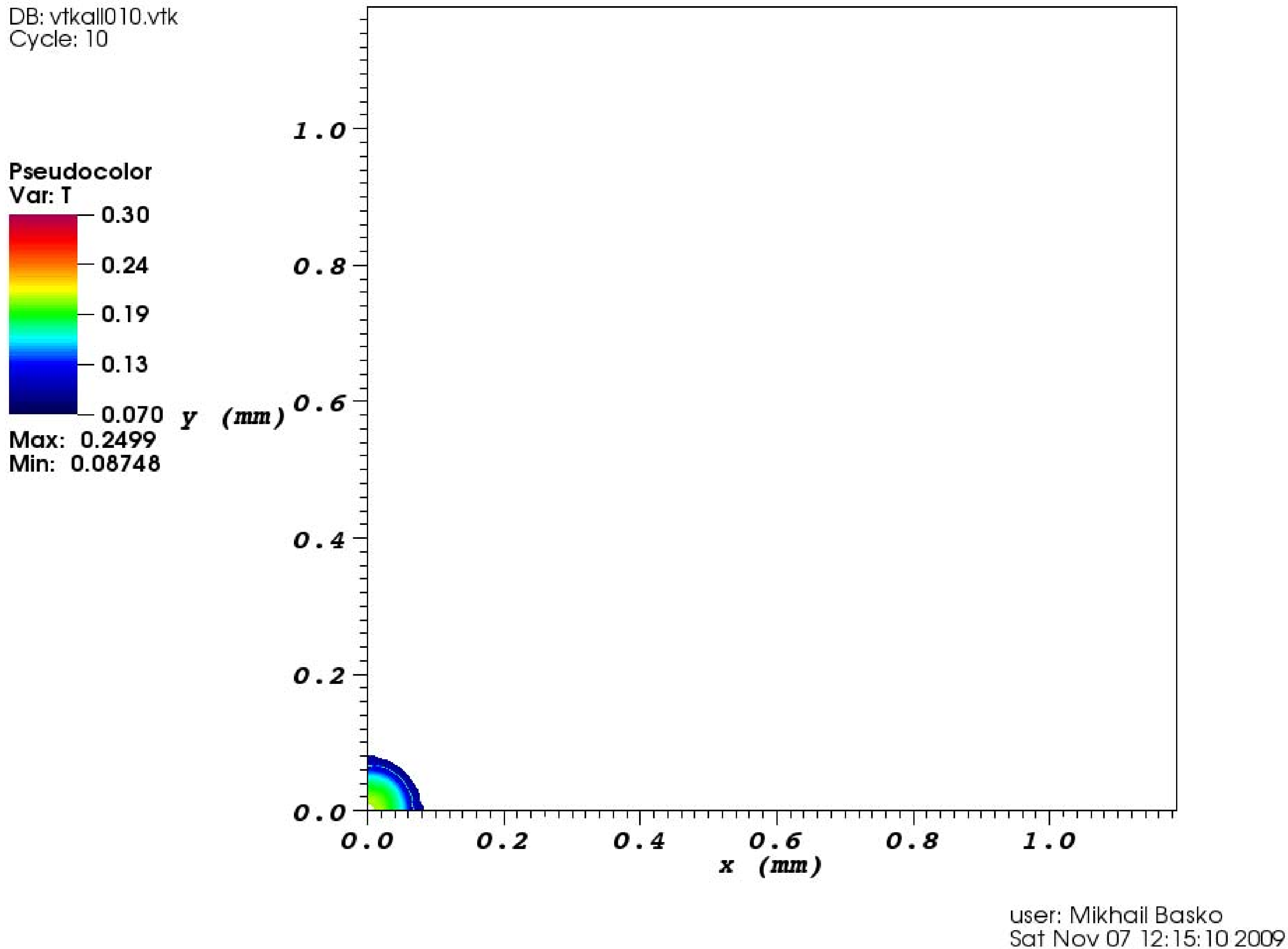
DB: vtkall010.vtk
Cycle: 10
Pseudocolor
Var: T
0.30
0.24
0.19
0.13
0.070
Max: 0.2499
Min: 0.08748
y (mm)
1.0
0.8
0.6
0.4
0.2
0.0
0.0
0.2
0.4
0.6
0.8
1.0
x (mm)
user: Mikhail Basko
Sat Nov 07 12:15:10 2009

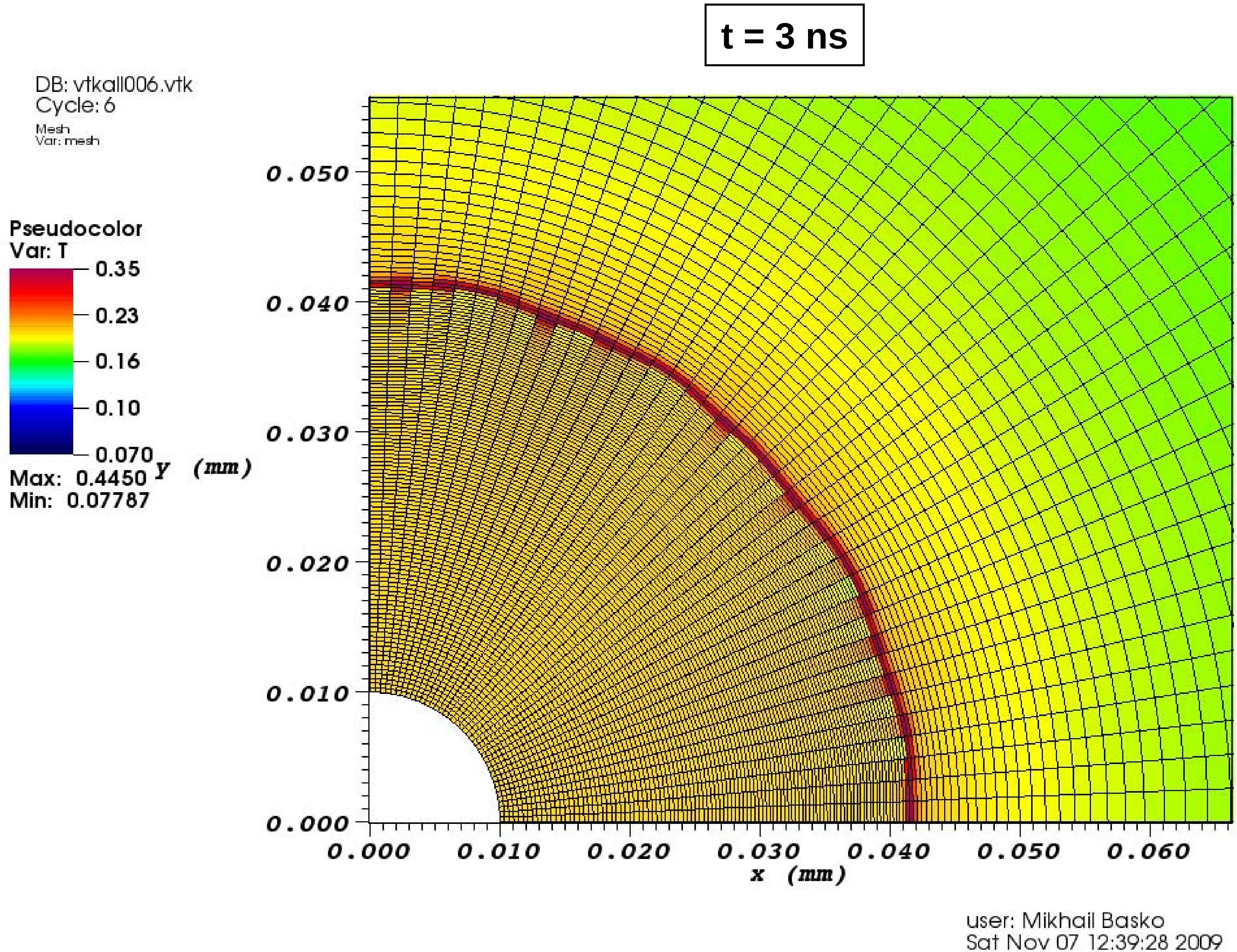
t = 3 ns
DB: vtkall006.vtk
Cycle: 6
Mesh
Var: mesh
Pseudocolor
Var: T
0.35
0.23
0.16
0.10
0.070
Max: 0.4450
Min: 0.07787
Y (mm)
0.050
0.040
0.030
0.020
0.010
0.000
0.000
0.010
0.020
0.030
0.040
0.050
0.060
x (mm)
user: Mikhail Basko
Sat Nov 07 12:39:28 2009

Shock structure

Here we deal with a radiation-dominated shock front, which has a supercritical amplitude (see Zel'dovich and Raizer, chapter VII). The shocked material radiates away about 90% of its initial kinetic energy.

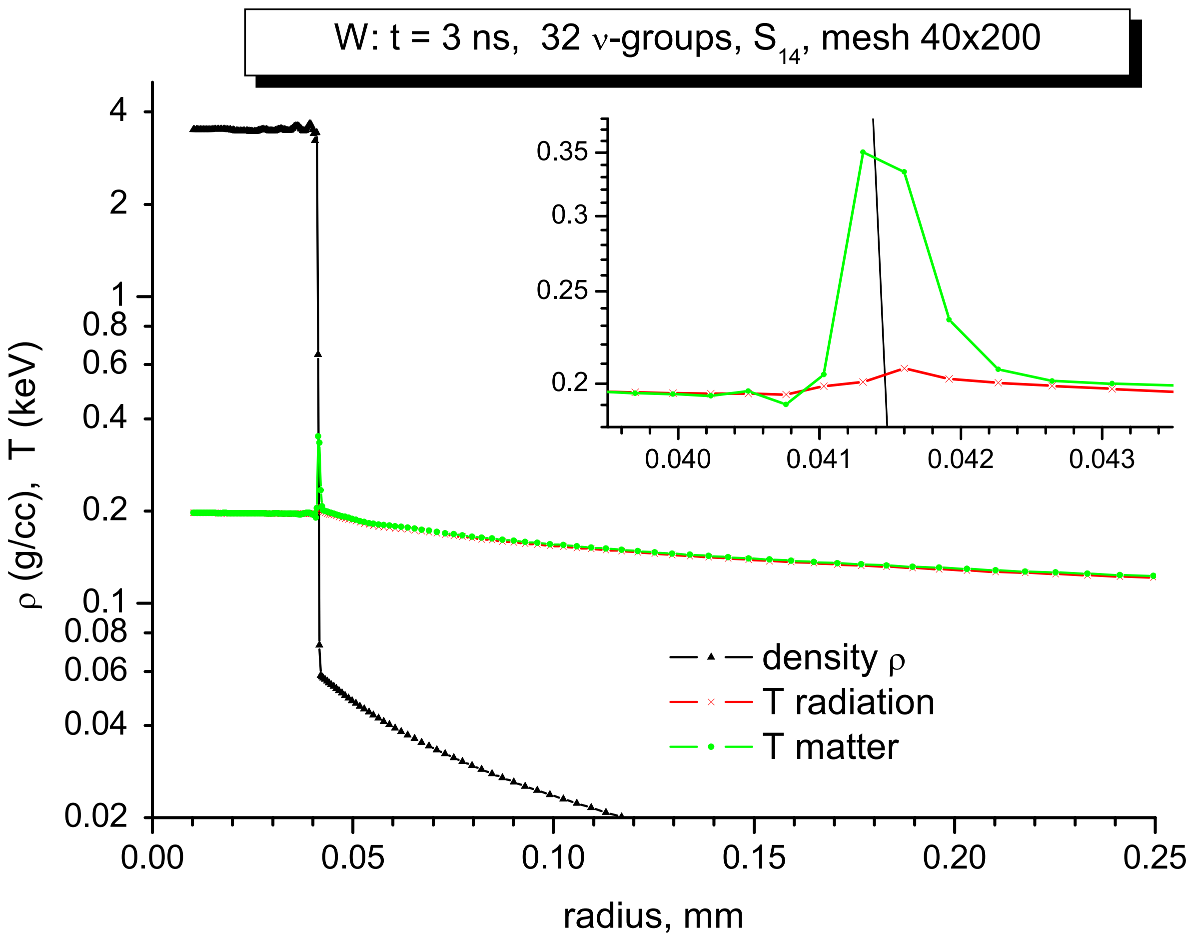

Plasma opacities

Plasma opacities for the above simulation have been provided by the group of V.G.Novikov from the Keldysh institute (KIAM) with the THERMOS code.

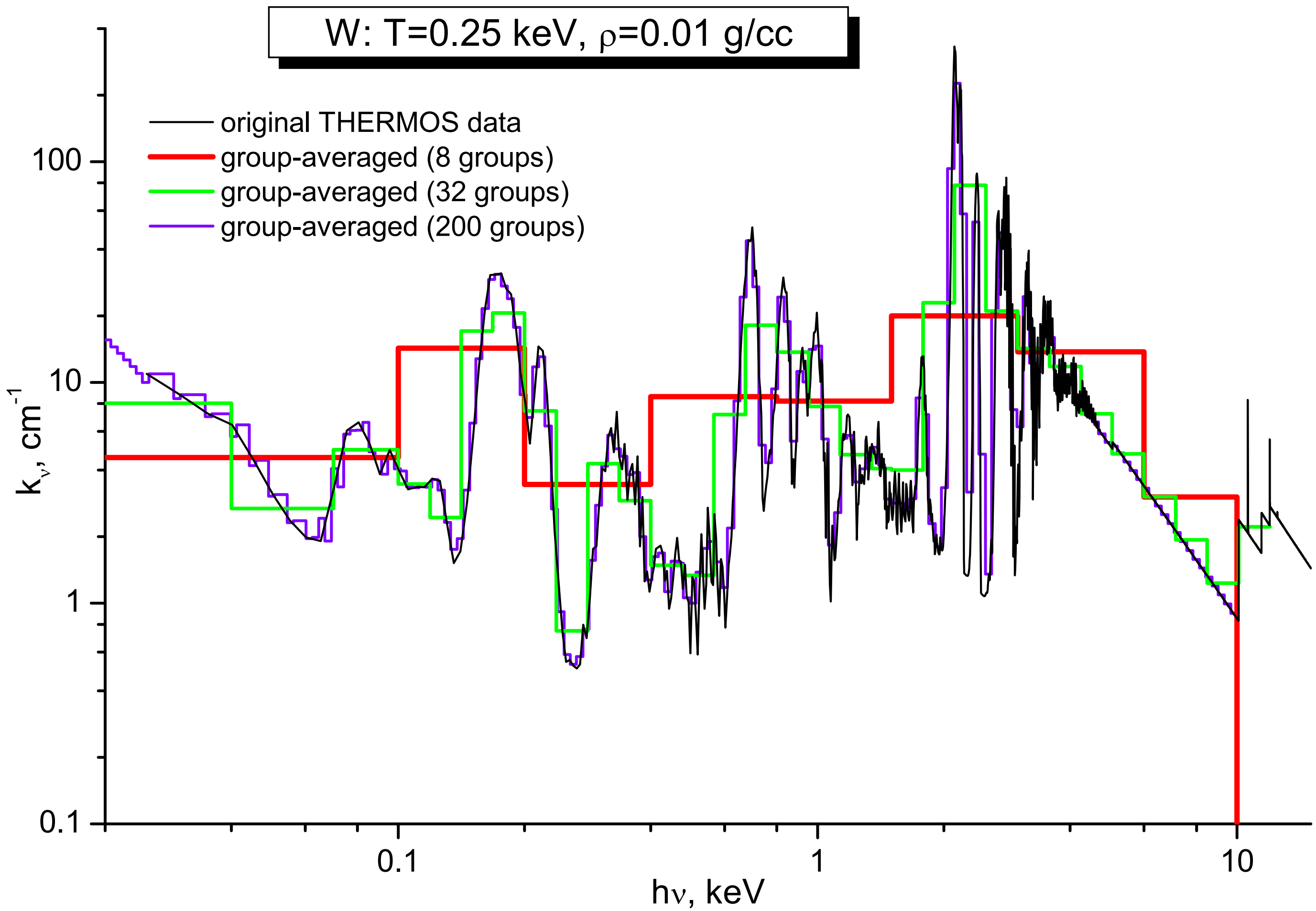

Total X-ray emission power

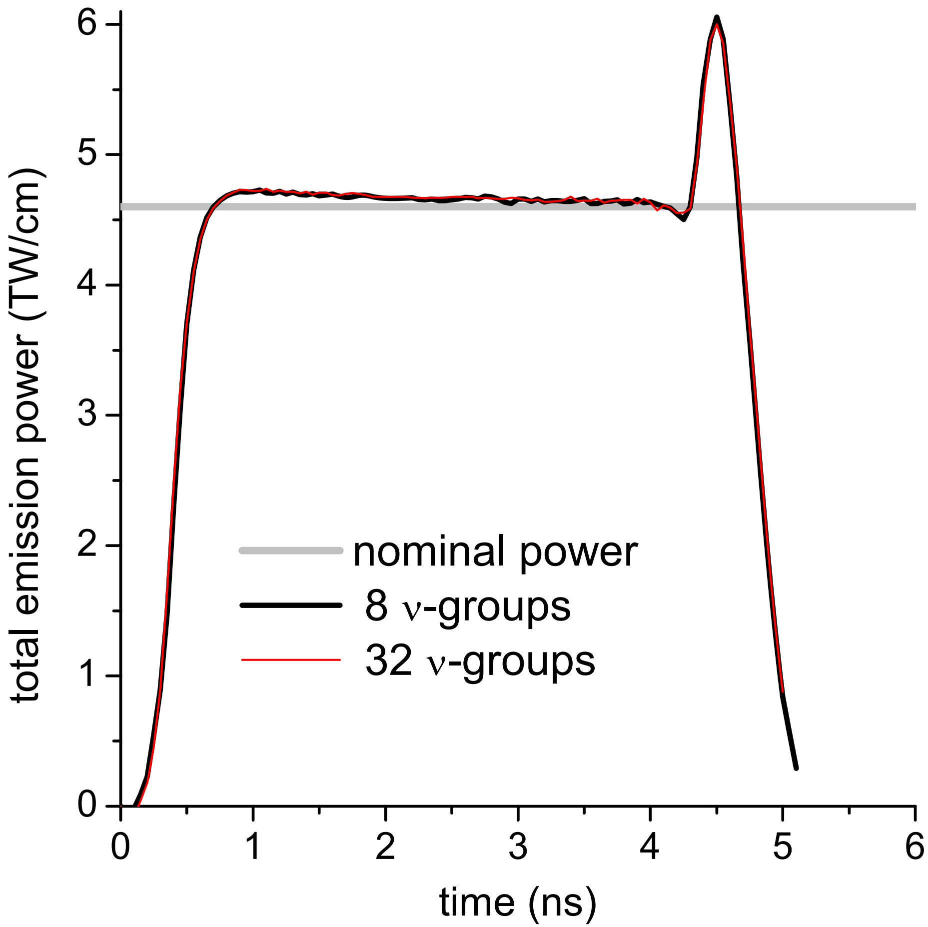

The imploding tungsten plasma radiates away about 90% of its initial kinetic energy.

The nominal power of implosion is

$$W_{nom} = \frac{1}{2} M U_{im}^2 / t_{pulse} =$$

$$= 23 \text{ kJ cm}^{-1} / 5 \text{ ns} = 4.6 \text{ TW cm}^{-1}$$

Spatially integrated emission spectra

High-resolution emission spectra can be obtained in the post-processor regime even when hydrodynamics is simulated with a relatively small number (~10) of spectral groups.

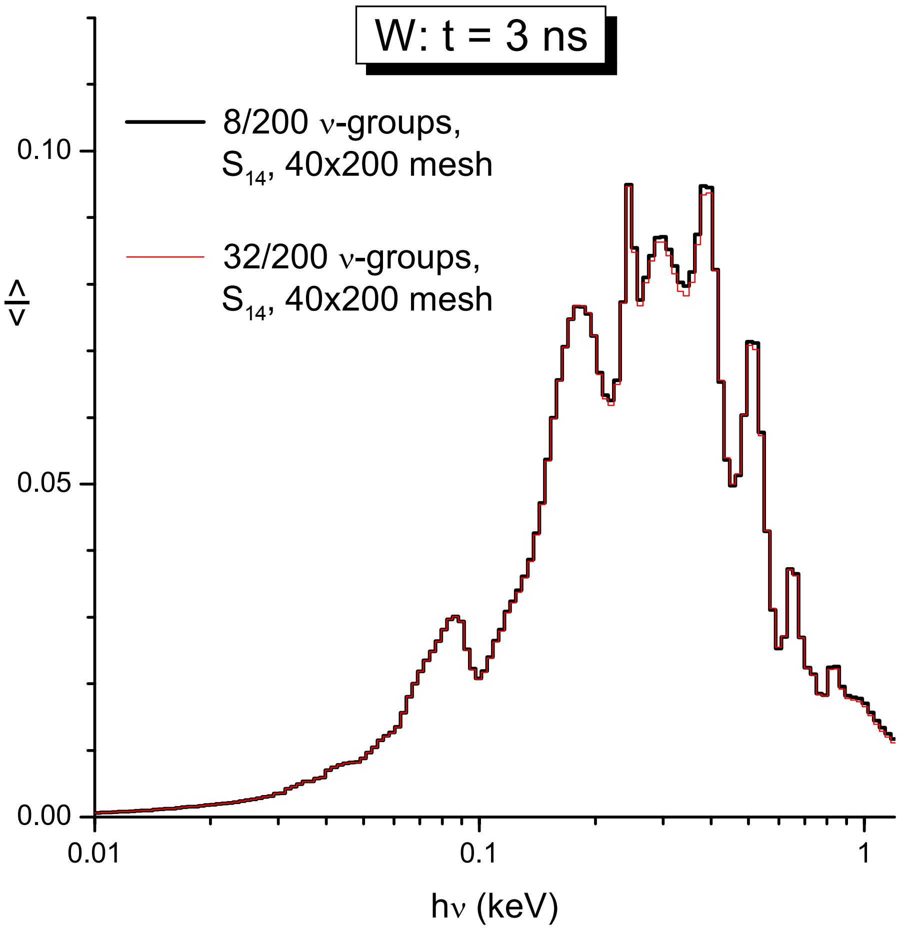

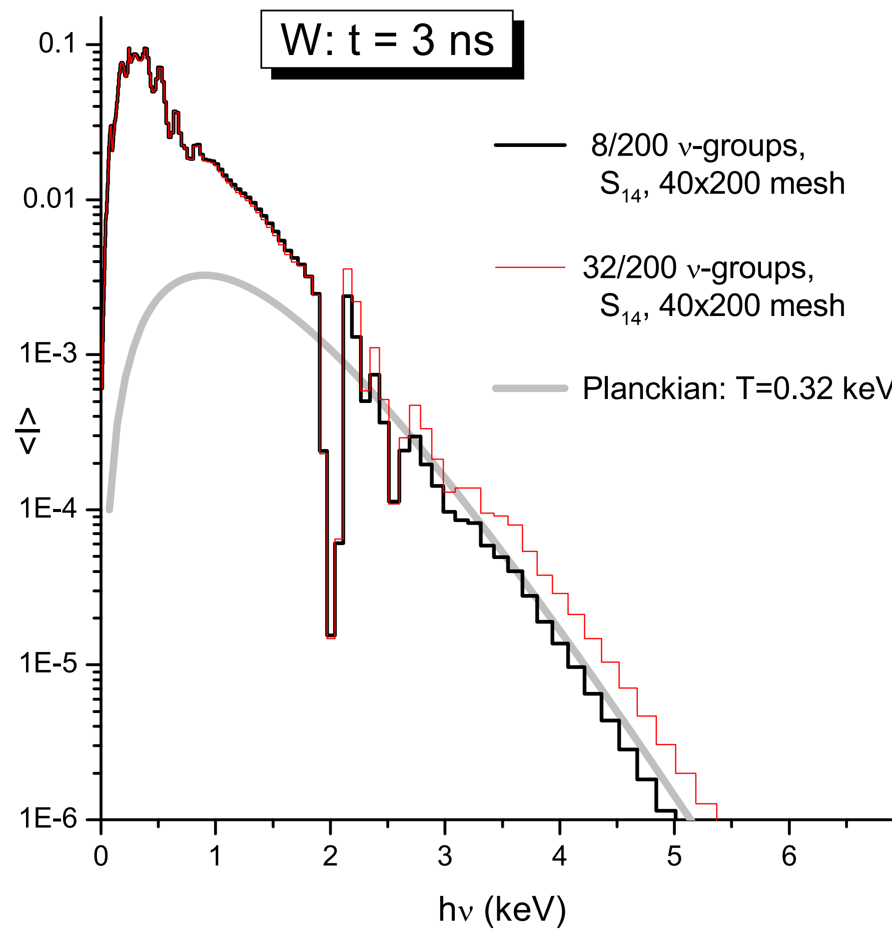

Optical thickness of the imploding plasma

Over a wide range of frequencies, the shock front lies at an optical depth of τ = 0.5–2.0

$\Rightarrow$ the multi-frequency diffusion is not an adequate approach for such situations!

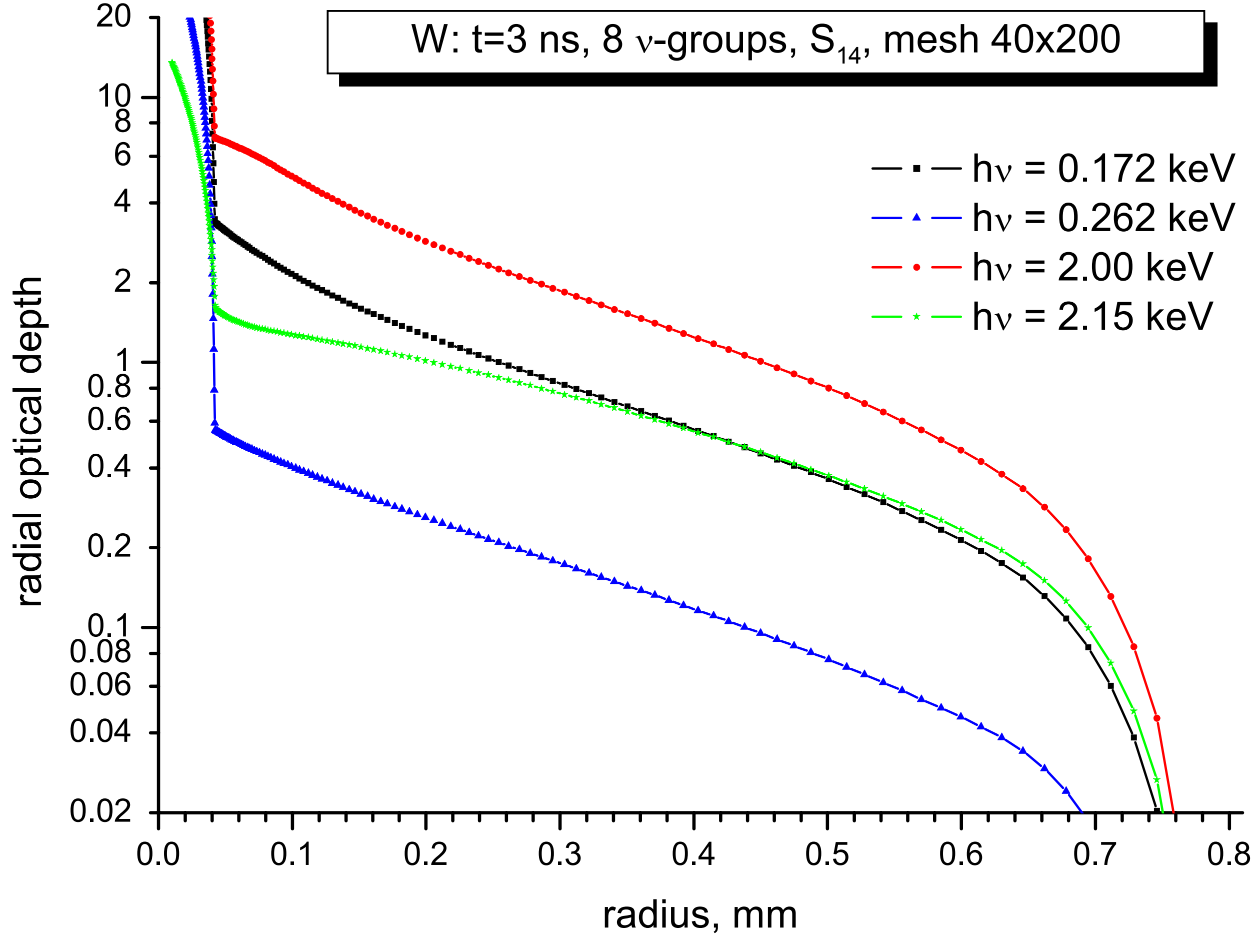

Calculated X-ray images of the central pinch

Spectral X-ray images provide information on the internal structure of the imploding pinch.

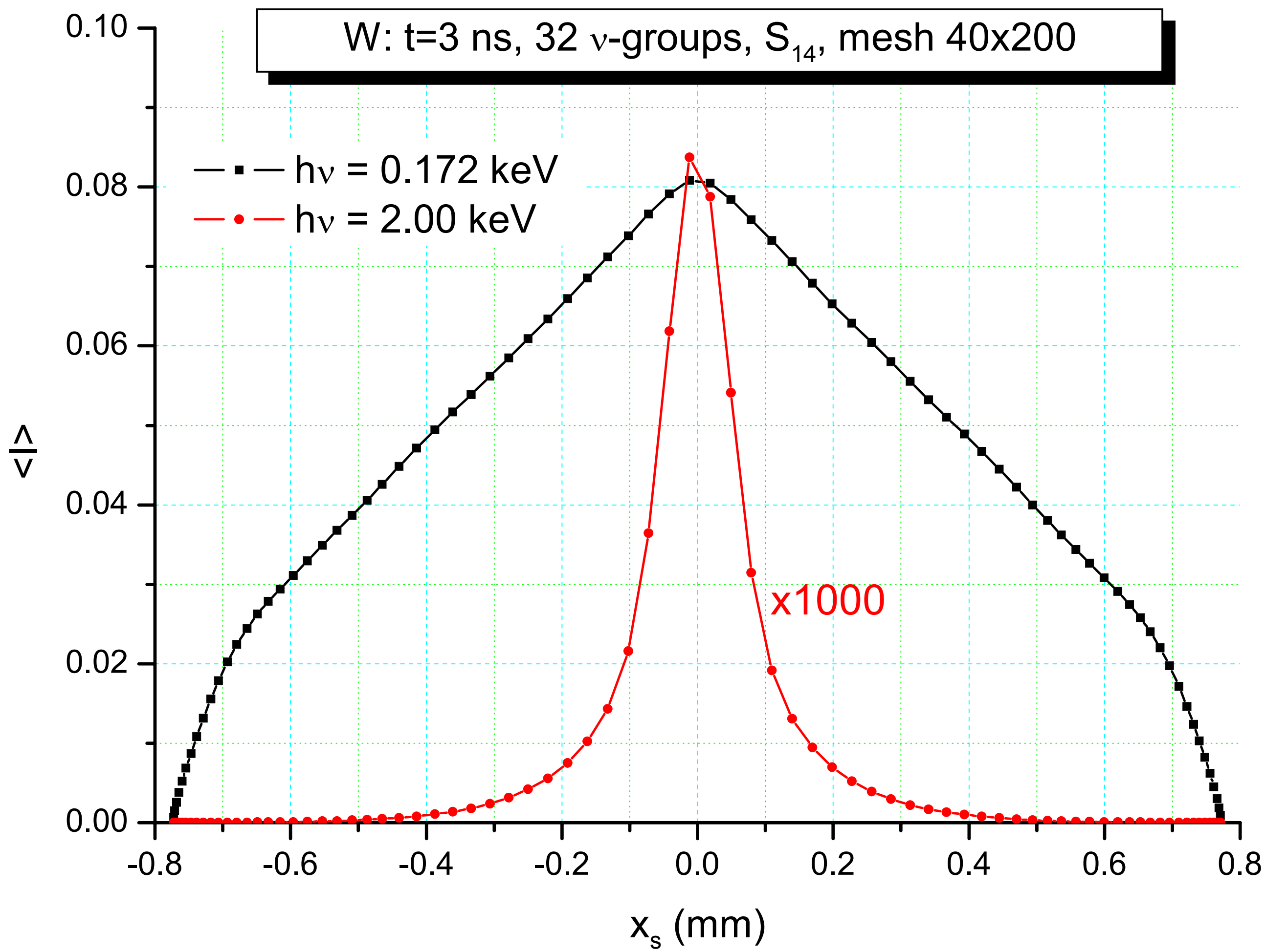

Problem 2: Hole boring in a copper foil by an intense nanosecond laser pulse

Copper foil under PHELIX (GSI) irradiation

Cu foil: $4 g/cc \times 2 \mu m = 0.8 mg/cm^2$, $T_0 = 0.58$ eV

PHELIX beam (prepulse): 2-3 ns with 2×10^{13} W/cm^2

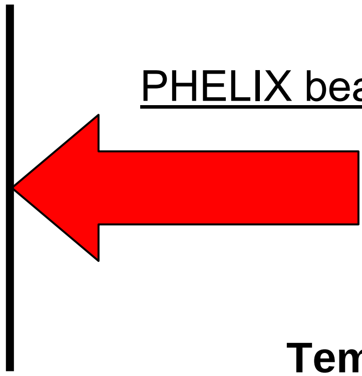

Temporal pulse profile

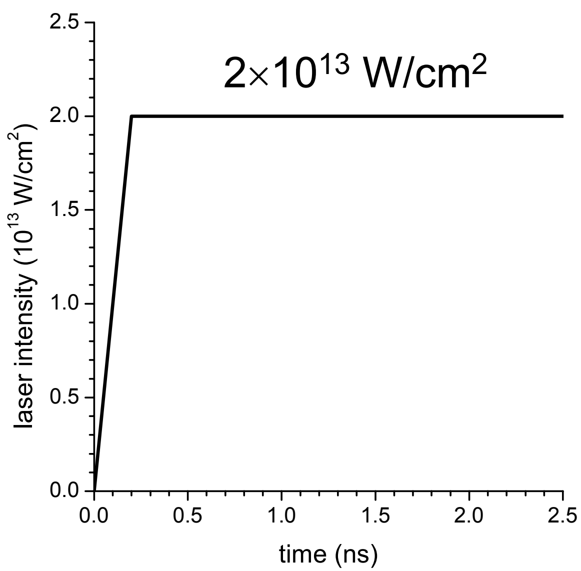

Spatial pulse profile

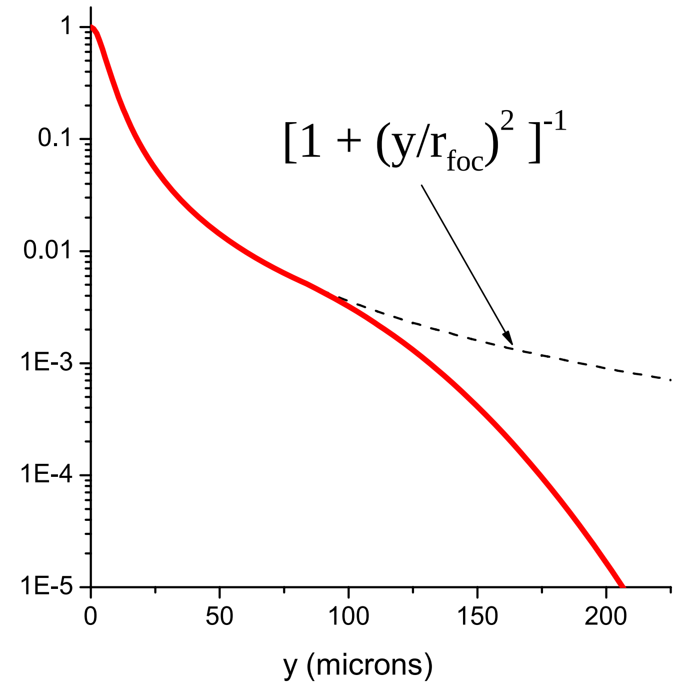

Simulation setup

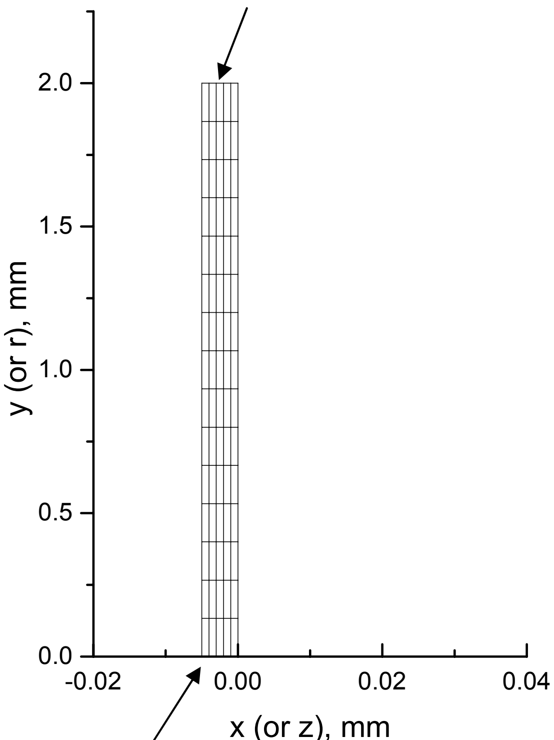

<u>Initial conditions:</u> ρ_0 = 4.0 g/cc, Δx = 2 μm, p_0 = 3 kbar, T_0 = 0.58 eV

<u>Boundary conditions:</u> p_b = 3 kbar

<u>EOS:</u> Novikov *et al.*

<u>Opacity:</u> Novikov *et al.*
9 freq. groups

<u>Laser deposition:</u> transport of one beam with the inverse bremsstrahlung absorption coefficient

<u>Mesh:</u> $n_x \times n_y = 150 \times 300$

<u>Spectral opacity of Cu</u>

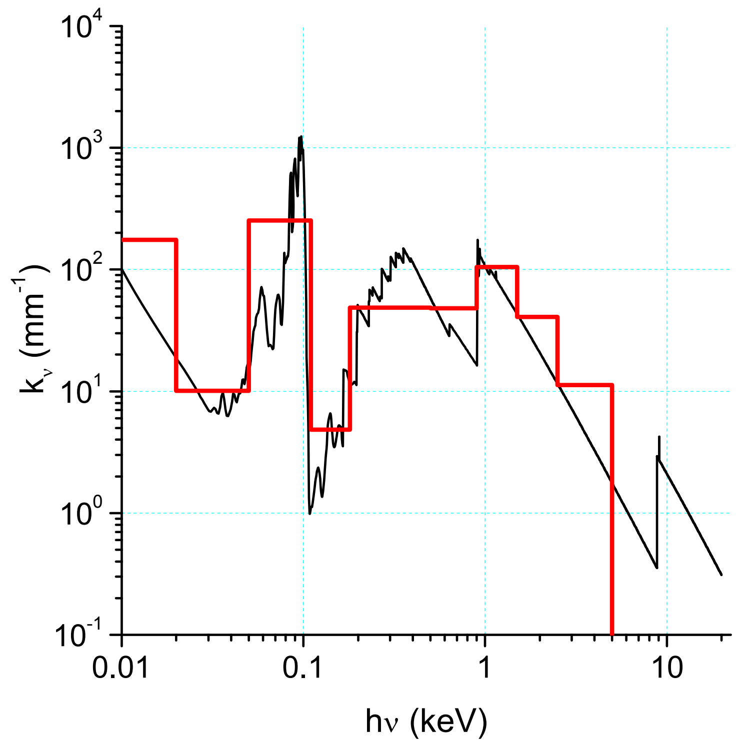

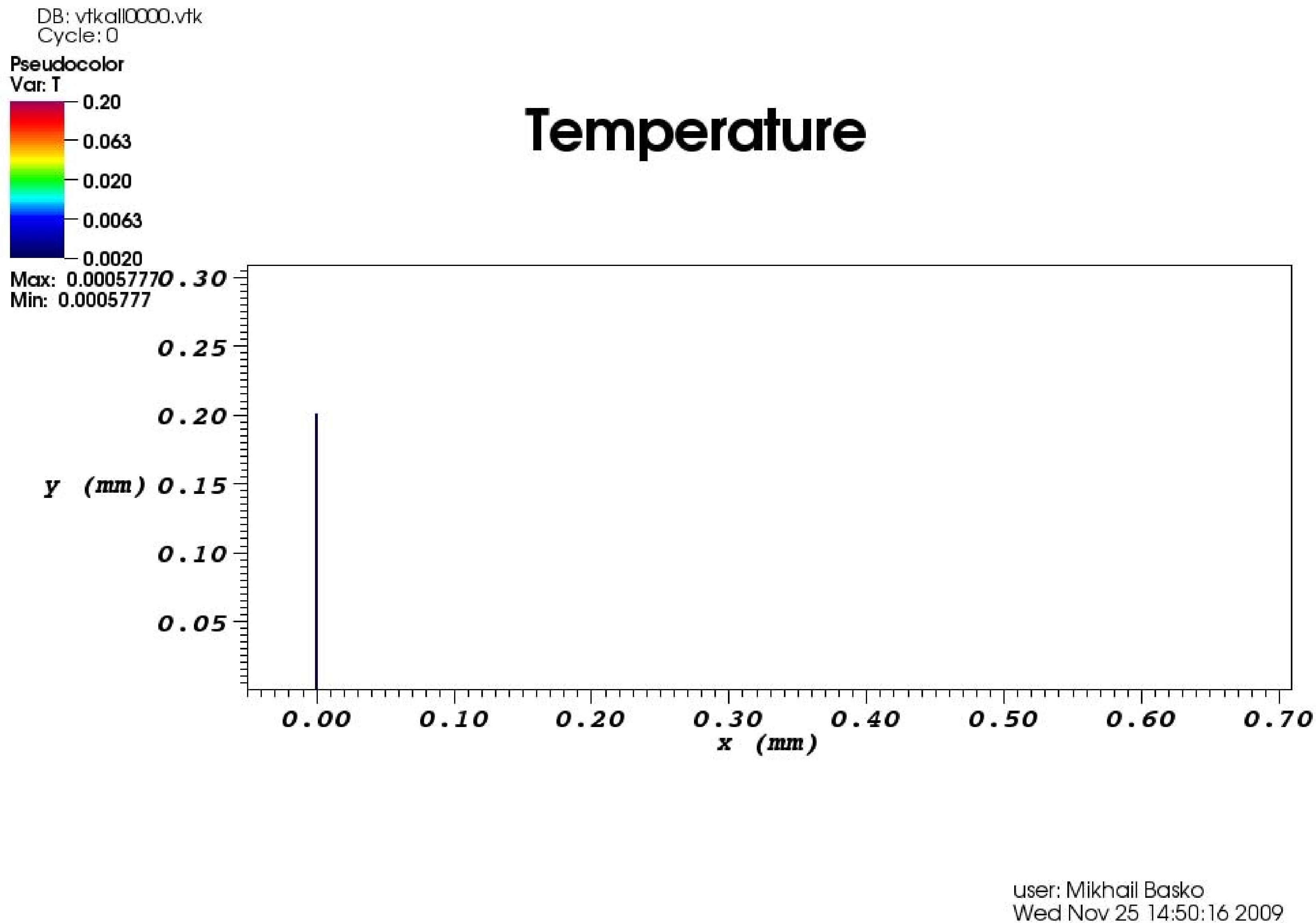
DB: vtkall0000.vtk
Cycle: 0
Pseudocolor
Var: T
0.20
0.063
0.020
0.0063
0.0020
Max: 0.0005777
Min: 0.0005777
Temperature
y (mm)
0.30
0.25
0.20
0.15
0.10
0.05
0.00
0.10
0.20
0.30
0.40
0.50
0.60
0.70
x (mm)
user: Mikhail Basko
Wed Nov 25 14:50:16 2009

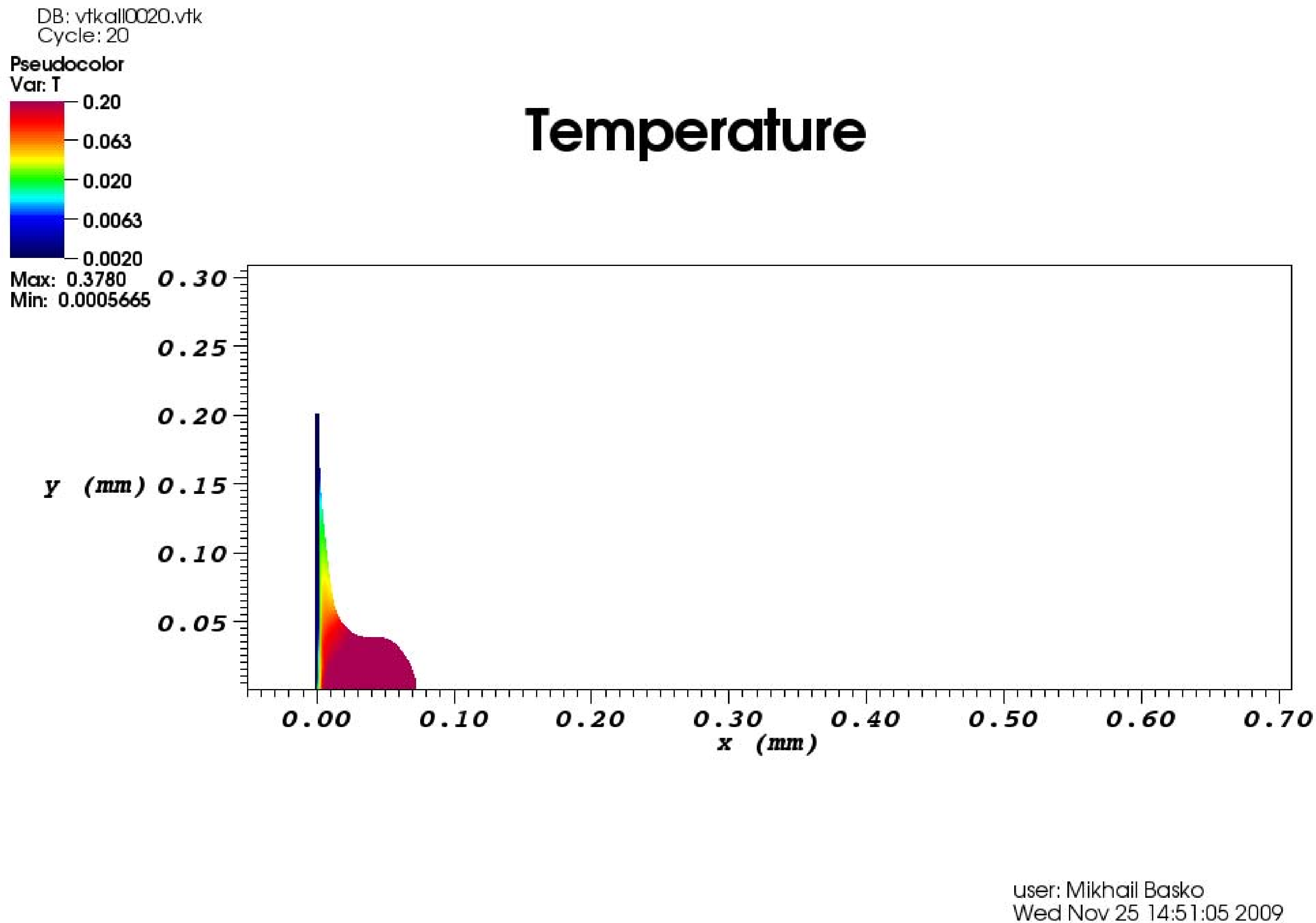
DB: vtkall0020.vtk
Cycle: 20
Pseudocolor
Var: T
0.20
0.063
0.020
0.0063
0.0020
Max: 0.3780
Min: 0.0005665
Temperature
y (mm)
0.30
0.25
0.20
0.15
0.10
0.05
0.00
0.10
0.20
0.30
0.40
0.50
0.60
0.70
x (mm)
user: Mikhail Basko
Wed Nov 25 14:51:05 2009

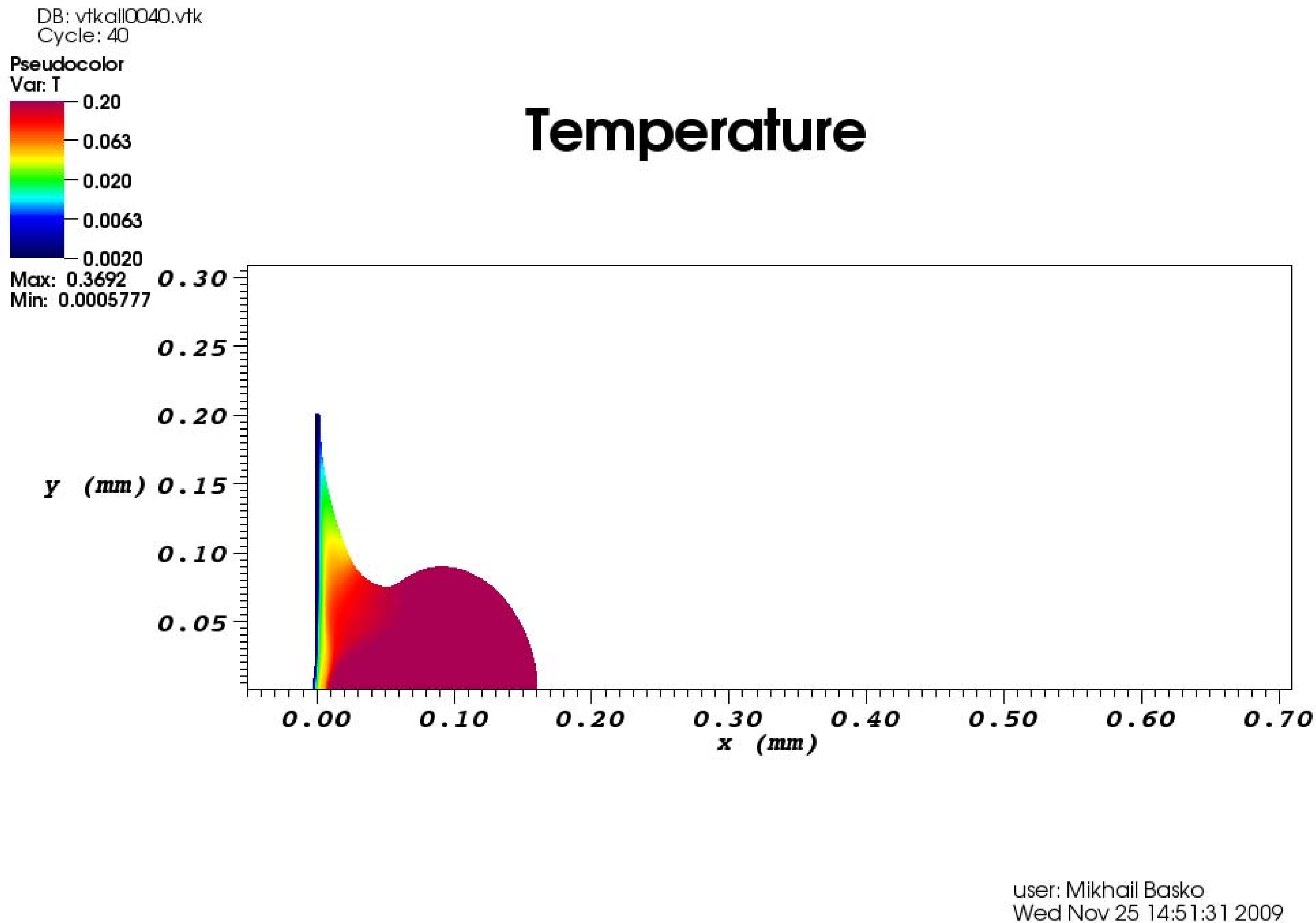
DB: vtkall0040.vtk
Cycle: 40
Pseudocolor
Var: T
0.20
0.063
0.020
0.0063
0.0020
Max: 0.3692
Min: 0.0005777
Temperature
0.30
0.25
0.20
0.15
0.10
0.05
y (mm)
0.00
0.10
0.20
0.30
0.40
0.50
0.60
0.70
x (mm)
user: Mikhail Basko
Wed Nov 25 14:51:31 2009

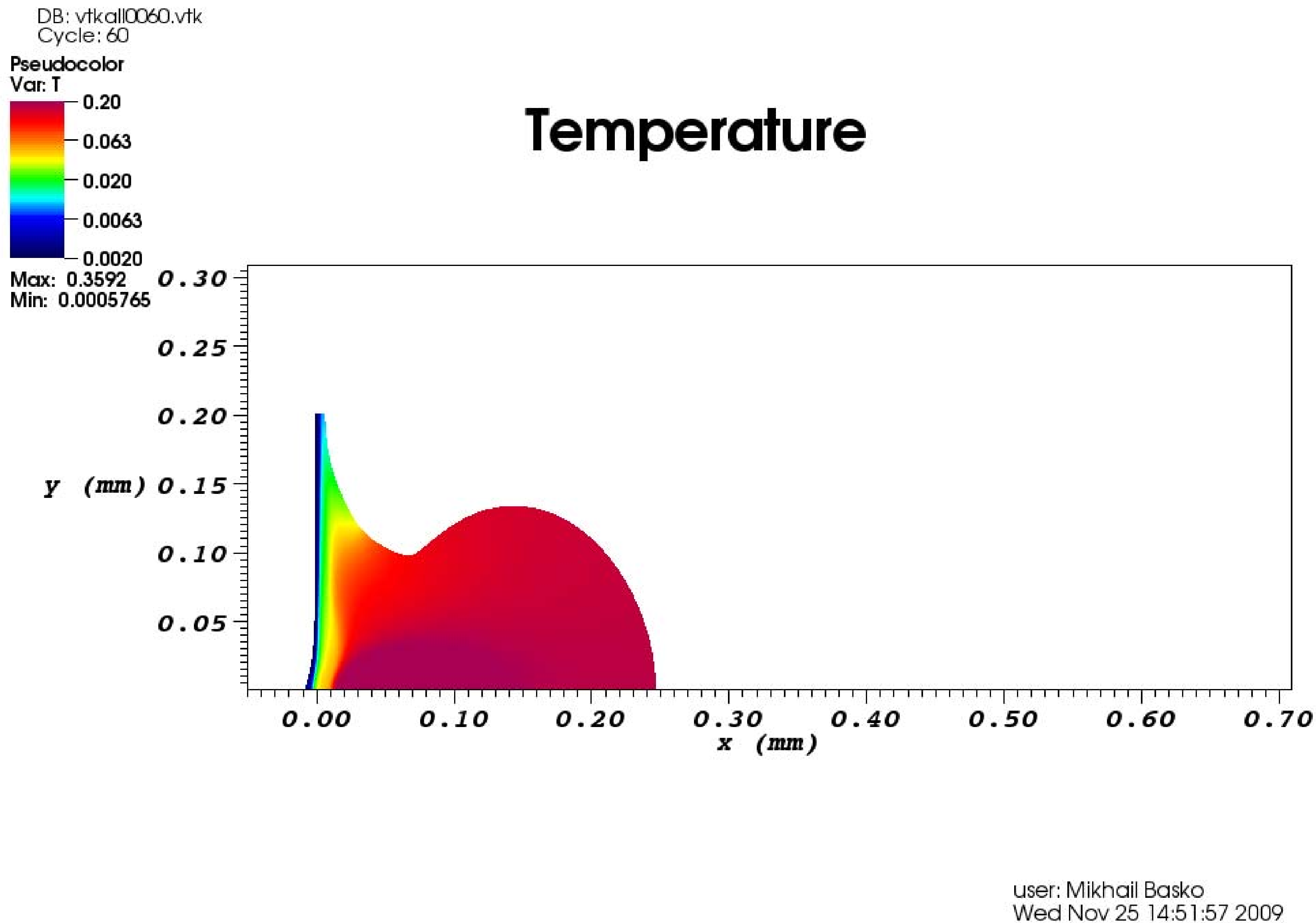
DB: vtkall0060.vtk
Cycle: 60
Pseudocolor
Var: T
0.20
0.063
0.020
0.0063
0.0020
Max: 0.3592
Min: 0.0005765
Temperature
y (mm)
0.30
0.25
0.20
0.15
0.10
0.05
0.00
0.10
0.20
0.30
0.40
0.50
0.60
0.70
x (mm)
user: Mikhail Basko
Wed Nov 25 14:51:57 2009

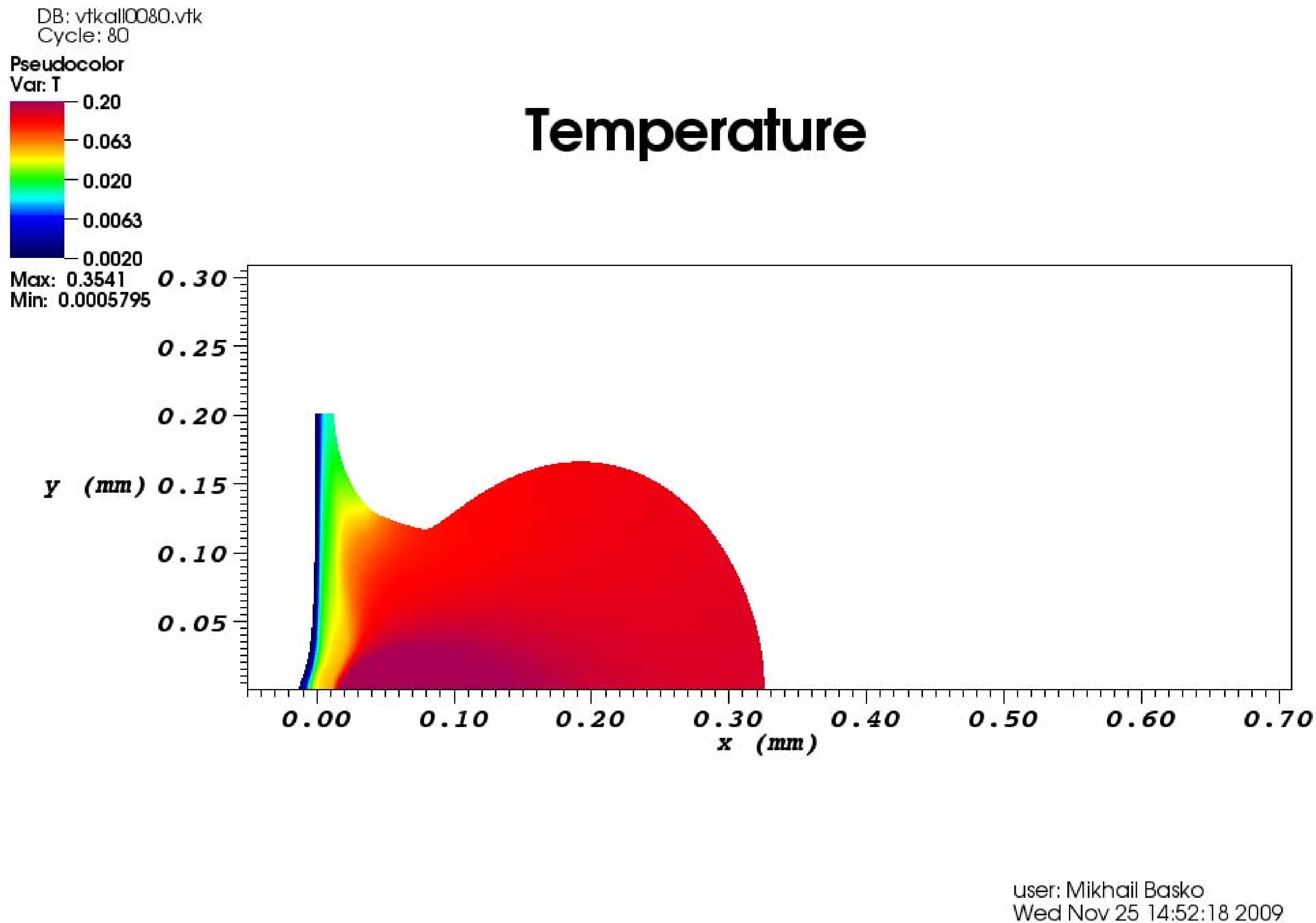
DB: vtkall0080.vtk
Cycle: 80
Pseudocolor
Var: T
0.20
0.063
0.020
0.0063
0.0020
Max: 0.3541
Min: 0.0005795
Temperature
0.30
0.25
0.20
0.15
0.10
0.05
y (mm)
0.00
0.10
0.20
0.30
0.40
0.50
0.60
0.70
x (mm)
user: Mikhail Basko
Wed Nov 25 14:52:18 2009

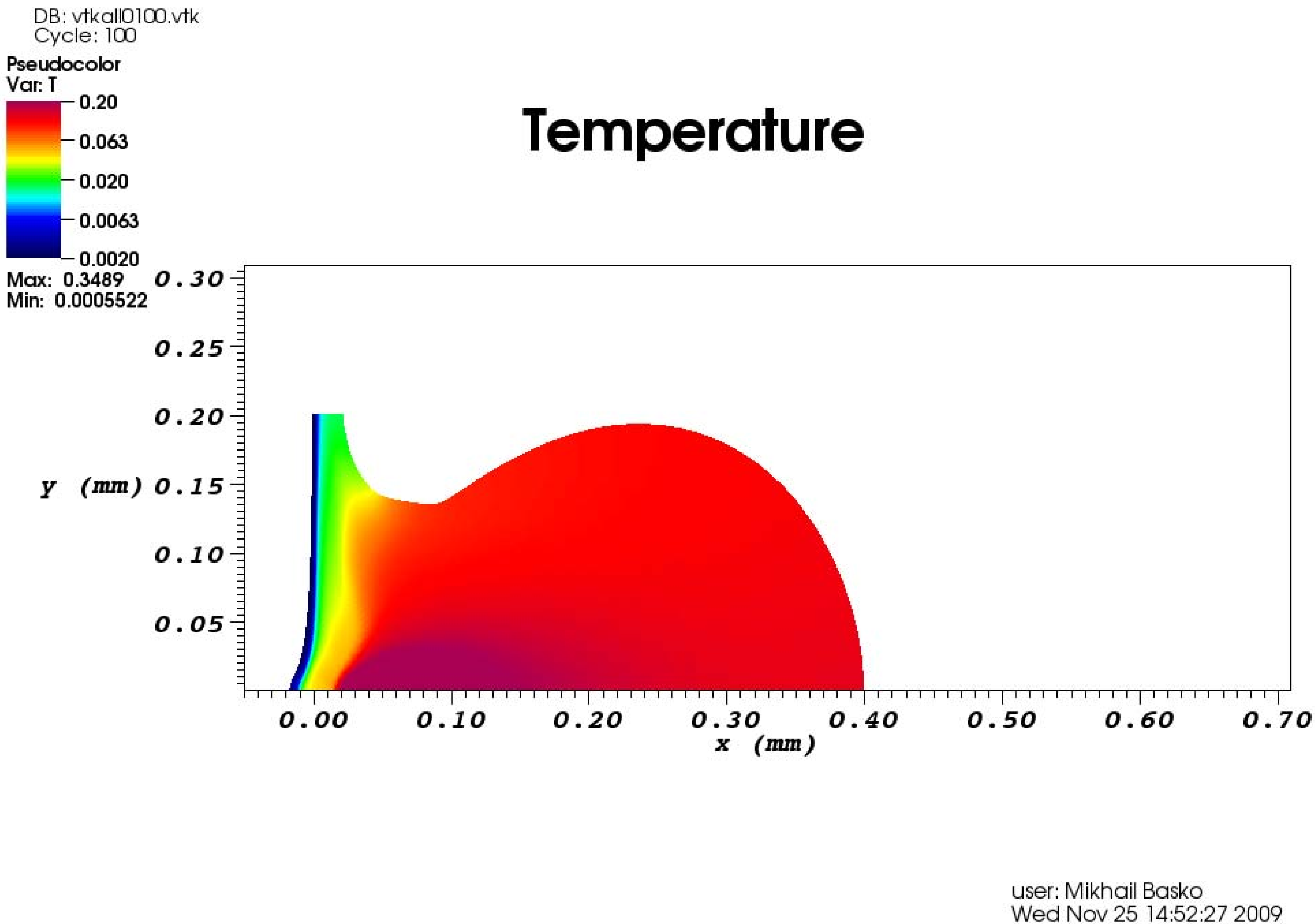
DB: vtkall0100.vtk
Cycle: 100
Pseudocolor
Var: T
0.20
0.063
0.020
0.0063
0.0020
Max: 0.3489
Min: 0.0005522
Temperature
0.30
0.25
0.20
0.15
0.10
0.05
y (mm)
0.00
0.10
0.20
0.30
0.40
0.50
0.60
0.70
x (mm)
user: Mikhail Basko
Wed Nov 25 14:52:27 2009

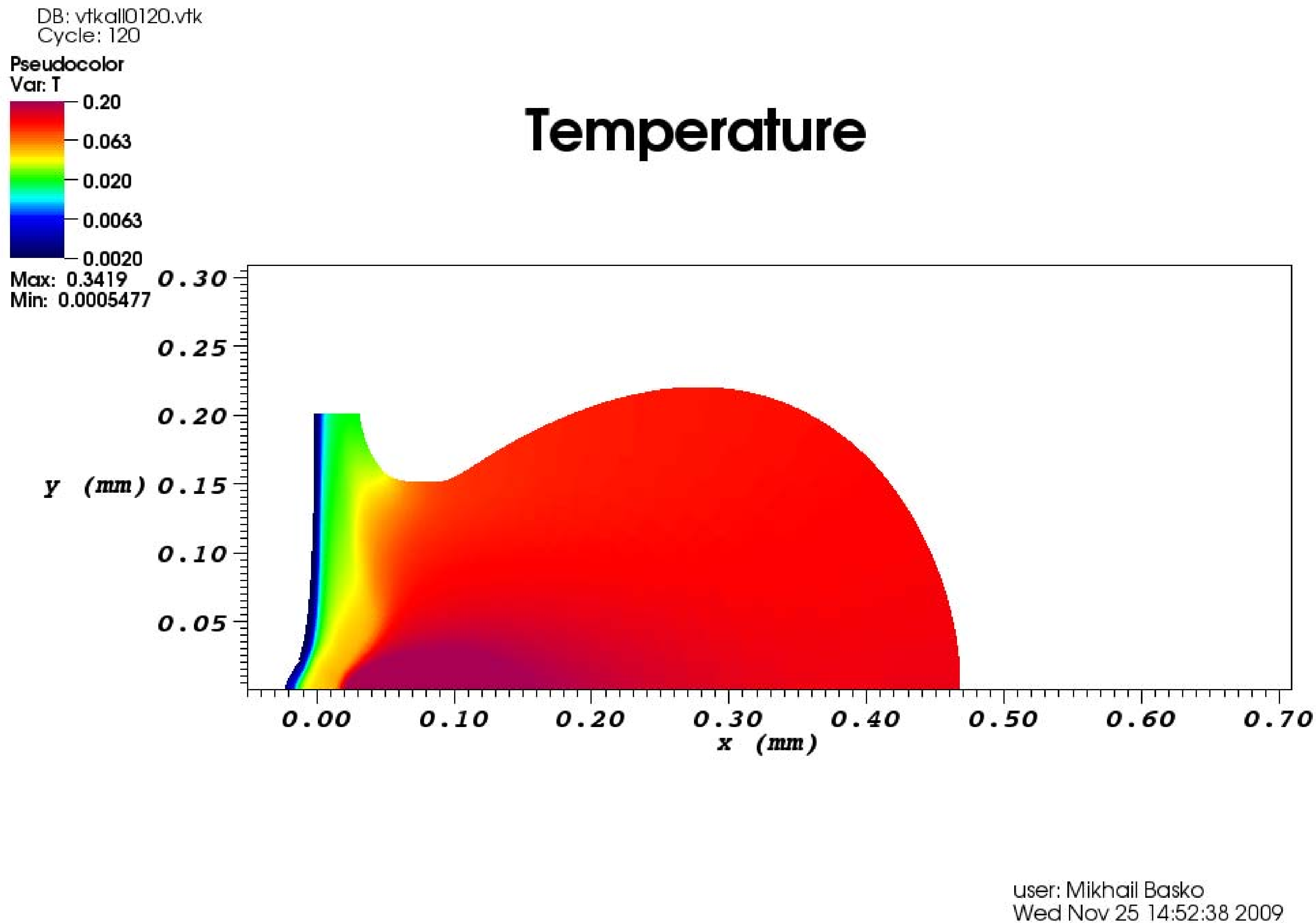
DB: vtkall0120.vtk
Cycle: 120
Pseudocolor
Var: T
0.20
0.063
0.020
0.0063
0.0020
Max: 0.3419
Min: 0.0005477
Temperature
y (mm)
0.30
0.25
0.20
0.15
0.10
0.05
0.00
0.10
0.20
0.30
0.40
0.50
0.60
0.70
x (mm)
user: Mikhail Basko
Wed Nov 25 14:52:38 2009

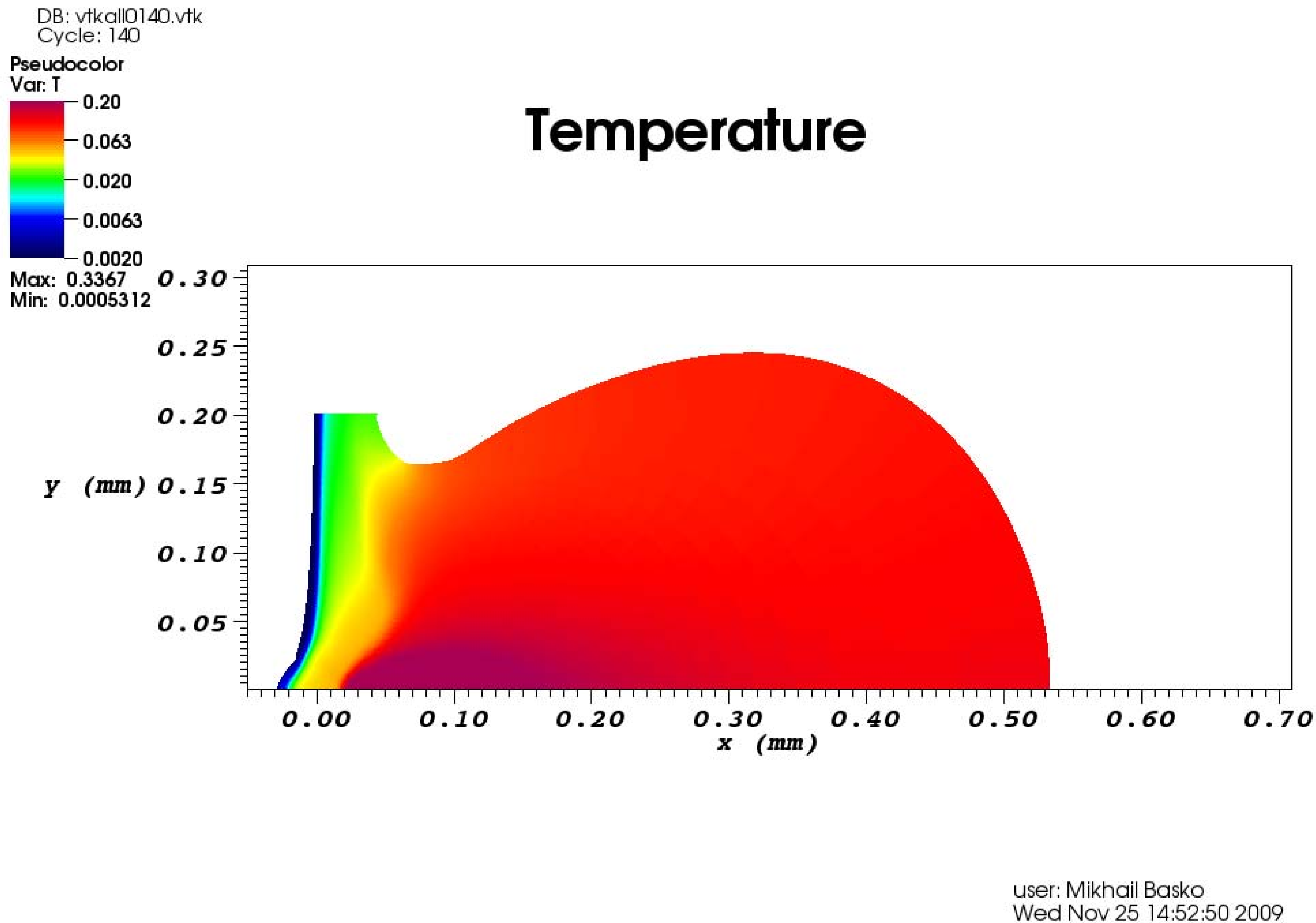

DB: vtkall0140.vtk
Cycle: 140
Pseudocolor
Var: T
0.20
0.063
0.020
0.0063
0.0020
Max: 0.3367
Min: 0.0005312
Temperature
y (mm)
0.30
0.25
0.20
0.15
0.10
0.05
0.00
0.10
0.20
0.30
0.40
0.50
0.60
0.70
x (mm)
user: Mikhail Basko
Wed Nov 25 14:52:50 2009

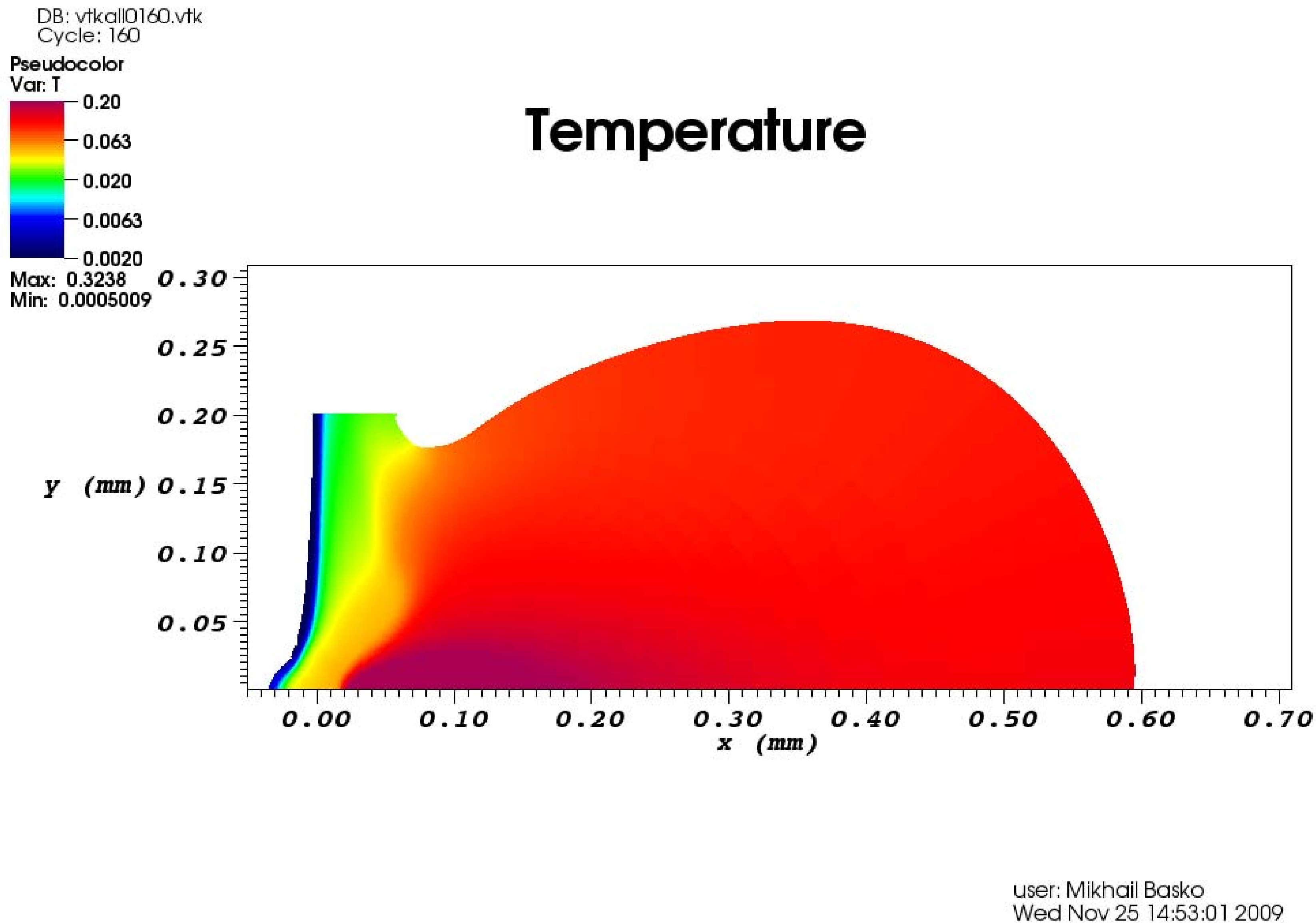
DB: vtkall0160.vtk
Cycle: 160
Pseudocolor
Var: T
0.20
0.063
0.020
0.0063
0.0020
Max: 0.3238
Min: 0.0005009
Temperature
y (mm)
0.30
0.25
0.20
0.15
0.10
0.05
0.00
0.10
0.20
0.30
0.40
0.50
0.60
0.70
x (mm)
user: Mikhail Basko
Wed Nov 25 14:53:01 2009

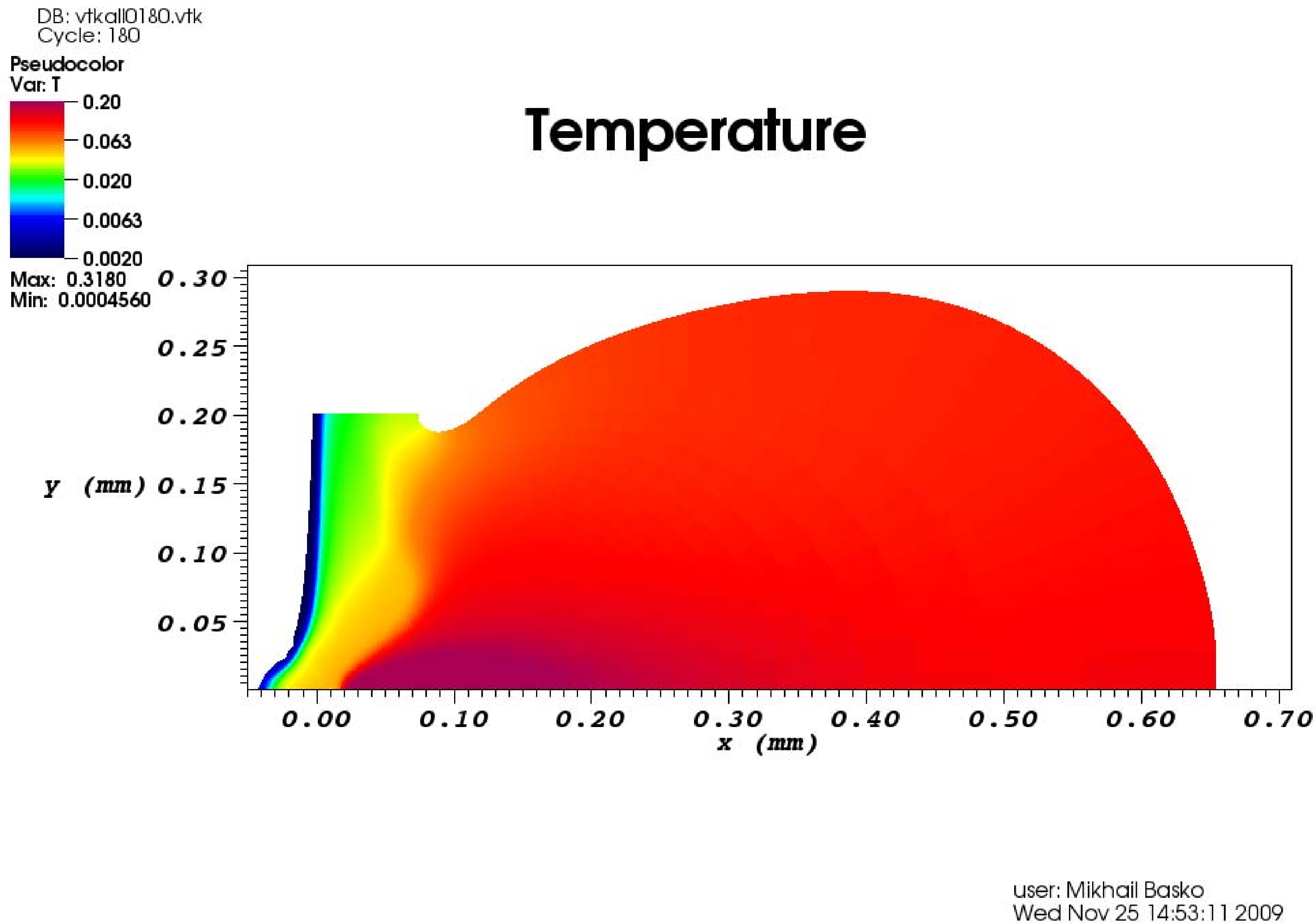
DB: vtkall0180.vtk
Cycle: 180
Pseudocolor
Var: T
0.20
0.063
0.020
0.0063
0.0020
Max: 0.3180
Min: 0.0004560
Temperature
y (mm)
0.30
0.25
0.20
0.15
0.10
0.05
0.00
0.10
0.20
0.30
0.40
0.50
0.60
0.70
x (mm)
user: Mikhail Basko
Wed Nov 25 14:53:11 2009

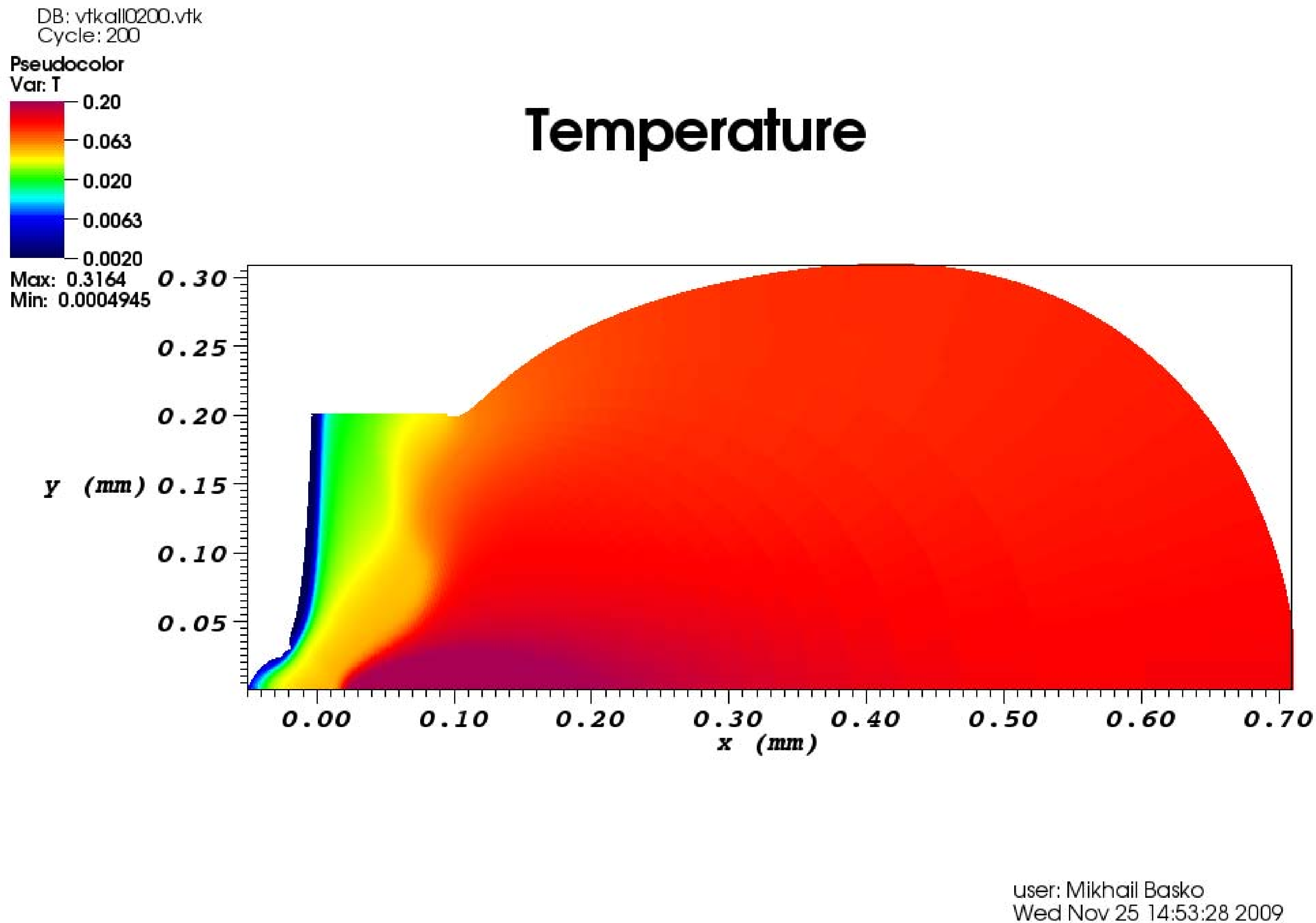
DB: vtkall0200.vtk
Cycle: 200
Pseudocolor
Var: T
0.20
0.063
0.020
0.0063
0.0020
Max: 0.3164
Min: 0.0004945
Temperature
y (mm)
0.30
0.25
0.20
0.15
0.10
0.05
0.00
0.10
0.20
0.30
0.40
0.50
0.60
0.70
x (mm)
user: Mikhail Basko
Wed Nov 25 14:53:28 2009

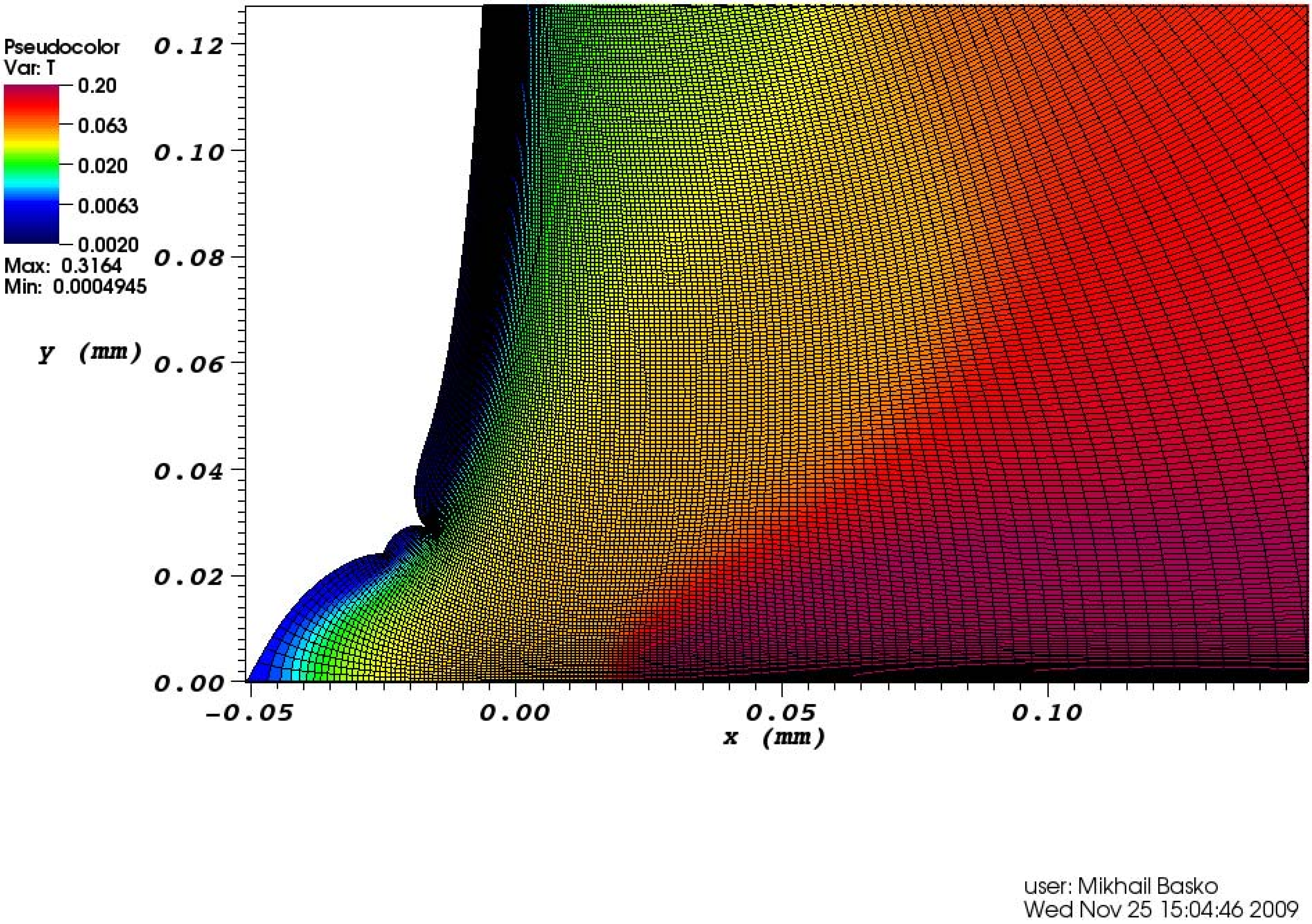
Pseudocolor
Var: T
0.20
0.063
0.020
0.0063
0.0020
Max: 0.3164
Min: 0.0004945
y (mm)
0.12
0.10
0.08
0.06
0.04
0.02
0.00
-0.05
0.00
0.05
0.10
x (mm)
user: Mikhail Basko
Wed Nov 25 15:04:46 2009

Effects of 2D expansion

Time dependence of mass column density $\int \rho \, dx$ **along the central axis at** $y = 0$ **.**

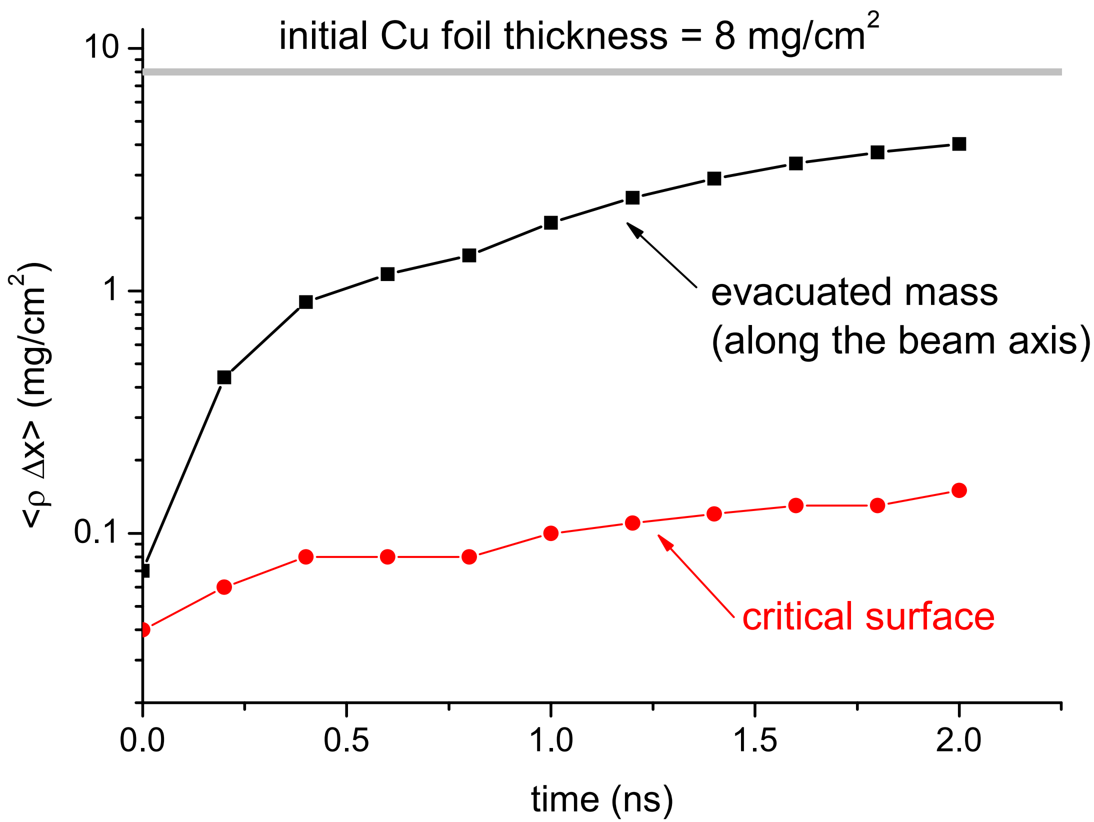

<u>The effect of hole boring</u>: the evacuated mass exceeds the depth of the critical surface by as large a factor as 20–30.

Conclusions

The status of the RALEF-2D code:

- the first results are encouraging,
- the work on further development continues.